J. Fluid Mech. (2000), *vol.* 408, *pp.* 1–38. Printed in the United Kingdom

A study of turbulence under conditions of transient flow in a pipe

By S. HE AND J. D. JACKSON

The School of Engineering, University of Manchester, Oxford Road, Manchester M13 9PL, UK

(Received 6 May 1997 and in revised form 10 September 1999)

A detailed investigation of fully developed transient flow in a pipe has been undertaken using water as the working fluid. Linearly increasing or decreasing excursions of flow rate were imposed between steady initial and final values. A three-beam, two-component laser Doppler anemometer was used to make simultaneous measurements of either axial and radial, or axial and circumferential, components of local velocity. Values of ensemble-averaged mean velocity, root-mean-square velocity fluctuation and turbulent shear stress were found from the measurements.

Being the first really detailed study of ramp-type transient turbulent flow, the present investigation has yielded new information and valuable insight into certain fundamental aspects of turbulence dynamics. Some striking features are evident in the response of the turbulence field to the imposed excursions of flow rate. Three different delays have been identified: a delay in the response of turbulence production; a delay in turbulence energy redistribution among its three components; and a delay associated with the propagation of turbulence radially. The last of these is the most pronounced under the conditions of the present study. A dimensionless delay parameter $\tau^+[= \sqrt{2}\tau U_{\tau 0}/D]$ is proposed to describe it. The first response of turbulence is found to occur in the region near the wall where turbulence production peaks. The axial component of turbulence responds earlier than the other two components and builds up faster. The response propagates towards the centre of the pipe through the action of turbulent diffusion at a speed which depends on the Reynolds number at the start of the excursion. In the core region, the three components of turbulence energy respond in a similar manner. Turbulence intensity is reduced in the case of accelerating flow and increased in decelerating flow. This is mainly as a result of the delayed response of turbulence. A dimensionless ramp rate parameter $\gamma[= (\mathrm{d}U_b/\mathrm{d}t)(1/U_{b0})(D/U_{\tau 0})]$ is proposed, which determines the extent to which the turbulence energy differs from that of pseudo-steady flow as a result of the delay in the propagation of turbulence.

1. Introduction

1.1. *General*

Apart from being of practical importance in connection with various engineering applications, the study of unsteady turbulent pipe flow is of value in providing information which can lead to an improved understanding of the phenomenon of turbulence. In such flows certain fundamental aspects of turbulent flow are exposed, which although present in steady turbulent flows are not apparent under such conditions. In addition, due to the effect of inertia, some additional features of turbulence specific to transient flows can be present. Due to the severe technical difficulties

involved, really detailed measurements of turbulence in transient flow were not possible until quite recently. As a result of the availability of modern instrumentation and powerful computers, transient turbulent flow can now be readily investigated. Accordingly, such flows have begun to receive more extensive study.

1.2. *Periodic pulsating flows*

Unsteady turbulent pipe flows can be conveniently classified into two groups, namely periodic pulsating flows and non-periodic transient flows. Pulsating turbulent pipe flow has received particular attention because of its practical importance and the ease with which it can be generated. Studies of this type of flow include those of Mizushina, Maruyama & Shiozaki (1973) and Mizushina, Maruyama & Hirasawa (1975), who used an electrochemical method, Shemer & Wygnanski (1981), Shemer & Kit (1984), Shemer, Wygnanski & Kit (1985), and Burnel, Raelison & Thomas (1990, 1991), who used hot wires, and Ramaprian & Tu (1980, 1983) and Tardu, Binder & Blackwelder (1994), who used single-component laser Doppler anemometry (LDA) systems. The fundamental variables involved in pulsating pipe flow are the amplitude and frequency of the imposed unsteadiness and the mean flow rate. In the studies mentioned, it has been found that whereas the effects on the velocity and turbulence fields of frequency of the oscillation and mean flow-rate can be significant, the effect of amplitude is small.

In addition to the Stokes number $D\sqrt{\omega/8\nu}$, where D is pipe diameter, ω is radian frequency and ν is kinematic viscosity, which has been widely used in the case of laminar flows, a number of other non-dimensional similarity parameters have been suggested for use in the case of pulsating pipe flow. Ramaprian & Tu (1983) used $\omega D/U_\tau$, where U_τ is friction velocity, when considering turbulent diffusion. Using this parameter and the Reynolds number based on mean flow rate, they classified pulsating turbulent pipe flow into five regimes. The Stokes–Reynolds number, $l_s^+ = l_s U_\tau/\nu$ (in which $l_s = \sqrt{2\nu/\omega}$ is the thickness of the viscous Stokes layer), was used by Binder & Kueny (1981), Binder *et al.* (1985) and Tardu *et al.* (1994). This parameter provides a measure of how far the viscous Stokes layer extends into the inner region of a turbulent flow. The parameter $\omega^+ (= \omega\nu/U_\tau^2)$ used by Mao & Hanratty (1986) is directly related to the Stokes–Reynolds number through $\omega^+ = 2/l_s^{+2}$. It will be seen later in the present paper that the diffusion of turbulence and the spread of the viscous Stokes layer are both important features of non-periodic transient turbulent flow.

In addition to the various experimental studies, computational modelling has been attempted by a number of researchers. The simplest turbulence model used involved prescribed distributions of eddy viscosity, see for instance Ohmi *et al.* (1976), Ohmi, Kyomen & Usui (1978), Kita, Adachi & Hirose (1980) and Shemer & Wygnanski (1981). A variety of one-equation turbulence models have been tried (Murphy & Prenter 1981; Cook, Murphy & Owen 1985; Ramaprian & Tu 1983 and Kirmse 1979) and also some two-equation models (Cousteix, Javelle & Houdeville 1981; Blondeaux & Colombini 1985). The resulting simulations have generally been found to be in poor agreement with experiment. However, recent investigations by the present authors and colleagues, using a number of low-Reynolds-number k–ϵ models such as that of Launder & Sharma (1975), have met with more success (see, for instance, Cotton & Ismael 1991).

1.3. *Non-periodic turbulent flows*

In contrast to pulsating pipe flow, non-periodic transient pipe flow has received relatively little attention. The few studies of this kind undertaken so far have involved

a variety of types of imposed excursions of flow rate. An early investigation by Kataoka, Kawabata & Miki (1975) studied the start-up response to a step input of flow rate in a pipe using an electrochemical technique. The time at which transition from laminar to turbulent flow occurred was found to decrease with increase of the Reynolds number of the imposed flow. The study of Maruyama, Kuribayashi & Mizushina (1976) was concerned with transient turbulent pipe flow following a stepwise increase of flow rate from an initial steady turbulent flow condition. Delays were observed in the response of turbulence, which were found to be greater at the centre of the pipe than close to the wall.

Kurokawa & Morikawa (1986) studied flow transients with gradually increasing and decreasing flow rate in a pipe. Their study showed that the transition Reynolds number increased with ramp rate and that, even for a very small imposed acceleration, transition from laminar to turbulent flow was significantly postponed. In the case of laminar flow, the friction coefficient was found to be greater than the corresponding value for quasi-steady flow. In contrast, it was found to be smaller under conditions of turbulent flow.

The experimental study of Lefebvre (1987) was concerned with accelerating flow in a pipe. The experimental facility was equipped with advanced instrumentation, including a two-component LDA system and six flush-mounted hot-film sensors. Unfortunately, the measurements of turbulence reported were rather limited. Discussion was mainly concentrated on transition from laminar to turbulent flow based on results from single excursions. However, some ensemble-averaged information obtained from 20 repeated runs was also presented. The mean velocity profiles and turbulent intensity profiles both generally exhibited a quasi-steady variation, although a reduction in turbulence intensity was clearly evident at the beginning of some of the transients.

1.4. *Spatially accelerating and decelerating flows*

It is appropriate at this point to consider transient turbulent flow in relation to another type of non-equilibrium flow, namely spatially accelerating or decelerating flow. Comparisons can be made between the two with the aid of the concept of an equivalent convection velocity and, when this is done, it is found that they share some common features.

Early studies of turbulent boundary layers with streamwise pressure gradients include those of Kline *et al.* (1969), Patel & Head (1968), Narayanan & Ramjee (1969) and Blackwelder & Kovasznay (1972). It was found that turbulence was enhanced where the flow was decelerating. Under such conditions bursts of turbulence were more frequent and violent. In contrast, when the flow was accelerating, turbulence was generally attenuated and the bursting frequency was reduced. When the flow was accelerated sufficiently, the bursting process ceased, and reverse transition (sometimes referred to as relaminarization) occurred.

More recently, very comprehensive studies have been conducted on boundary layers subjected to favourable and adverse pressure gradients, in some cases coupled with streamwise curvature. These have yielded measurements of higher-moment turbulence quantities. Examples include Muck, Hoffmann & Bradshaw (1985), Baskaran, Smits & Joubert (1987), Webster, Degraaff & Eaton (1996) and Schwarz & Plesniek (1996). While convex curvature has been found to have an effect similar to that of flow acceleration, stabilizing the flow and attenuating turbulence, concave curvature has the opposite effect. Some of the features of such flows have been related by the investigators to the propagation of turbulence structures from the wall outwards.

Experimental studies of internal flows with spatial acceleration or deceleration have

been reported by Tanaka & Yabuki (1986), Sano & Asako (1993) and Spencer, Heitor & Castro (1993). Again turbulence has been found to be attenuated when the flow is accelerating and enhanced when it is decelerating.

1.5. *The present study*

Although much effort has been put into the study of unsteady turbulent flow, the understanding of turbulence under such conditions is far from complete. With the exception of the studies conducted by Shemer *et al.* (1985), who used a rake of nine hot wires, and Burnel *et al.* (1990, 1991), who used crossed hot-film probes, the majority of experimental studies of transient flow have involved only single-velocity-component measurements. Furthermore, attention has been concentrated mainly on the pulsating flow case, the emphasis being on using Fourier analysis to extract information about the phase angle and amplitude of the responses of the mean flow and turbulence.

The present study was undertaken with a view to adding to the information available on non-periodic accelerating and decelerating ramp-type flows. A test facility was designed to enable ramp-type excursions of flow rate to be imposed in a long pipe. The flow rate could be caused to increase or decrease linearly with time from an initial steady value to a new one during a prescribed period. A two-component laser Doppler anemometer system was used which enabled simultaneous measurements of axial and radial or axial and circumferential components of velocity to be made. The experimental arrangement was such that highly repeatable excursions of flow rate could be imposed, thus enabling reliable ensemble-averaged results to be obtained. In this paper, experimental results are presented which not only show how mean flow and turbulence respond to imposed transients but also provide new insight into turbulence dynamics.

1.6. *Similarity and scaling*

Representing the governing equations, initial conditions and boundary conditions in dimensionless form, three dimensionless groups emerge for the problem under consideration here as parameters which control similarity and enable scaling calculations to be made. These are the initial Reynolds number $Re_0(= U_{b0}D/\nu)$, the final Reynolds number $Re_1(= U_{b1}D/\nu)$ and a dimensionless ramp rate parameter, $\alpha[(= D^3/\nu^2)(\mathrm{d}U_b/\mathrm{d}t)]$, where U_{b0} and U_{b1} are respectively the initial and final bulk velocity. The velocity and turbulence fields at the start of the excursion and their initial response to an imposed excursion of flow rate are determined by the value of the initial Reynolds number. The value of the ramp rate parameter determines the extent to which the velocity and turbulence fields depart from those of pseudo-steady flow as a result of the imposed excursion of flow rate. The final Reynolds number is only relevant to the post-transient response. If it is arranged that the dimensionless groups Re_0, Re_1 and α are the same for two systems, complete dynamical similarity will be achieved. The behaviour observed in one system can then be used to predict the response of the other, even though some or all of the variables ν, D, U_{b0}, U_{b1} and $\mathrm{d}U_b/\mathrm{d}t$ might be different.

By varying slightly the approach to representing the problem in non-dimensional form, a different dimensionless ramp rate parameter is obtained,

$$\beta = \frac{D}{U_{b0}^2}\left(\frac{\mathrm{d}U_b}{\mathrm{d}t}\right). \tag{1}$$

This is simply α divided by Re_0^2 and can therefore be used as an alternative to α for the purpose of scaling. It is of interest to note that β can be expressed as the ratio of

a time scale for the initial flow D/U_{b0} and a time scale associated with the imposed excursion $U_{b0}/(\mathrm{d}U_b/\mathrm{d}t)$. Pursuing this idea further and replacing D/U_{b0} by $D/U_{\tau 0}$, which as will be seen later, is a characteristic time scale associated with turbulent diffusion, a further dimensionless ramp rate parameter can be defined,

$$\gamma = \frac{D}{U_{\tau 0}} \left(\frac{1}{U_{bo}} \frac{\mathrm{d}U_b}{\mathrm{d}t} \right). \tag{2}$$

It can easily be shown that this parameter can be expressed as α multiplied by a function of Re_0 and, therefore, it too can be used as an alternative scaling parameter. As will be explained later γ has special relevance to turbulence behaviour in the particular non-periodic transient flows under consideration here because it provides an indication of the extent to which turbulence in ramp-type transient flow is likely to differ from that under conditions of pseudo-steady flow. If γ is very much less than unity, the flow will at all times have a turbulence structure similar to that of steady pipe flow at the current value of flow rate. We will describe such a flow as 'pseudo-steady transient pipe flow'. However, if γ is greater than unity, the flow will have a turbulence structure which differs markedly from that of steady pipe flow and the response of turbulence to the initiation of the flow rate excursion will be significantly delayed. The mean velocity field will also be modified. The bigger the value of γ the greater will be the departure from the pseudo-steady state.

2. Experimental investigation

2.1. *Flow loop and test section*

The experiments reported here were carried out using a test section which was a straight pipe of inside diameter 50.8 mm and length 9 m in which fully developed flow was achieved. Water was used as the working fluid. The closed circuit arrangement shown in figure 1 was employed. The flow was driven through the test section by the constant head difference between the two tanks. Flow control was achieved by adjusting the resistance using the pneumatically operated, computer-controlled valve situated downstream of the test section. A turbine flow meter placed in series with the flow control valve was used to measure the flow rate.

The test section consisted of a long length of polyvinyl chloride followed by a 2 m length of precision bore glass tube (wall thickness 2 mm). Both were very smooth internally and the inside diameters were carefully matched so that the junction between them was flush. A honeycomb flow straightener situated at the inlet to the test section was used to reduce any initial swirl. Fully developed flow could be expected at the transparent section with such an arrangement. Five carefully prepared pressure tappings were installed at equal intervals along the test section. The pressure differences between the tappings were measured using a precision differential pressure transducer of capacitance type.

2.2. *Laser Doppler anemometer*

A three-beam, two-component laser Doppler anemometer system utilizing frequency trackers was used to make simultaneous measurements of both axial and radial, or axial and circumferential, components of the velocity field. The forward scatter mode of operation was chosen in order to take advantage of the strength of the light scattered in this direction. The system was assembled from standard DANTEC optical components and electronic modules.

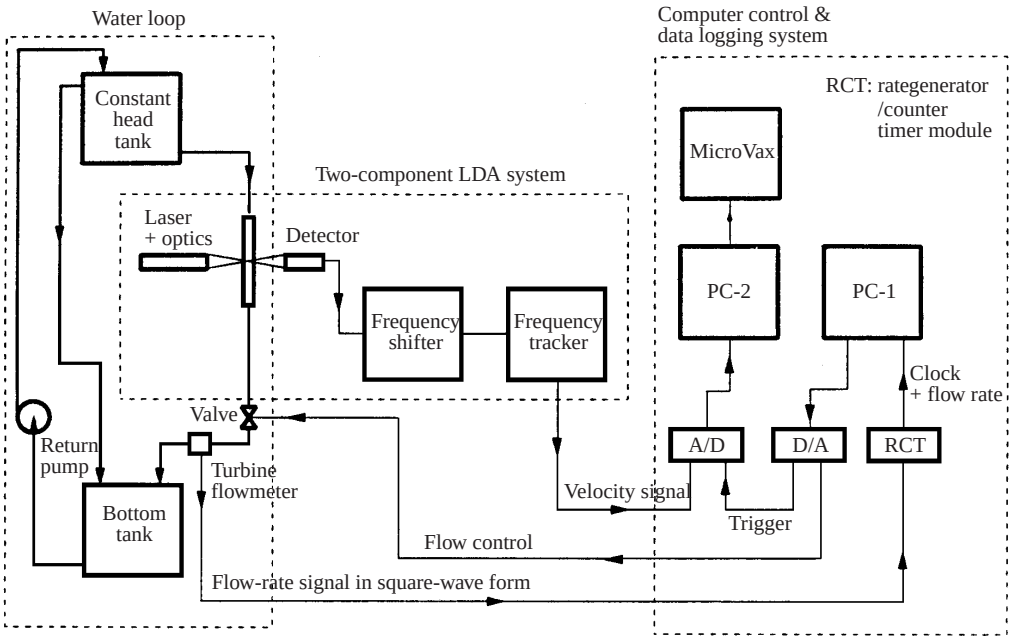

FIGURE 1. Experimental apparatus.

An arrangement of the beams was chosen which gave the velocity components in the directions $\pm 45^\circ$ to the axis of the pipe. The vertical and horizontal velocity components were calculated using the signals from the two channels. This arrangement has two advantages over an arrangement involving direct measurement of the vertical and horizontal components. Firstly, as the signals from the two channels are similar in magnitude and both are strong, the effects of electronic noise during processing and transmitting are similar in each case and relatively small. Also, with signals of similar magnitude, the performance of the PCI fast AD convertor is improved. Secondly, the symmetric arrangement of the beams allowed measurements to be made much closer to the wall than would otherwise have been possible.

The glass section of tube was surrounded by a transparent box of square cross-section filled with water. This helped to overcome difficulties due to the curvature of the wall and so improved the near-wall measurements. An arrangement whereby the photomultiplier was used off-alignment with the laser beam was found to help in significantly reducing the noise caused by reflections from the wall. The angle was varied between 5° and 15° to the x-axis when making measurements. The glass section was demounted and cleaned regularly to remove any dirt which settled on the wall.

The position of the measuring volume along the x-axis was chosen using the method proposed by Oldengarm, Krieken & Klooster (1975). They suggested that when the measuring volume reached the wall, light scattered from the particles attached to the wall would generate a sine wave signal. The amplitude of this bias frequency signal is a maximum when the centre of the measuring volume coincides with the wall surface. The wall position chosen this way was subsequently checked by exploring the symmetry of the mean velocity distribution. Initially, the position of the measuring volume along the y-axis was chosen by looking at the reflected beam from the far sidewall of the test section tube. The reflection would fail to follow the incident route if the incident beam was off the x-axis radius of the pipe, as shown in figure 2(a).

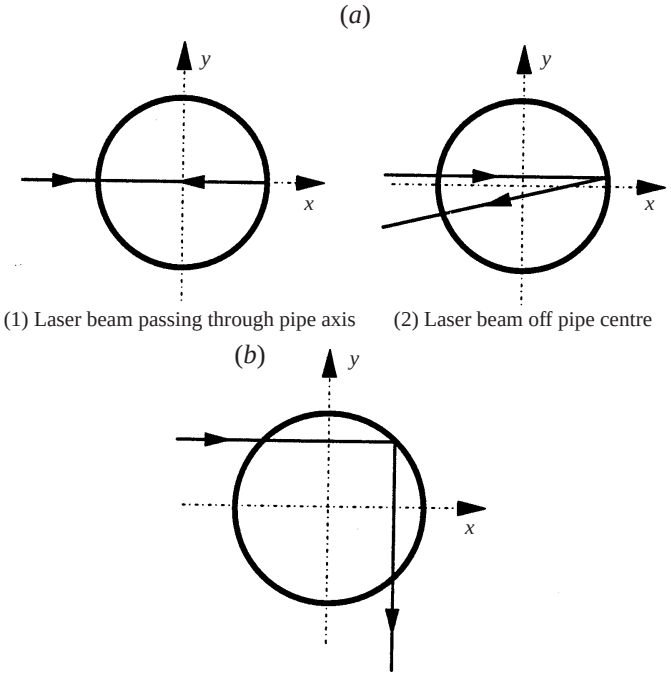

FIGURE 2. Determination of position of measuring volume in the y-direction.

A second approach was used in which the measuring volume was moved halfway between the centre and the wall of the tube. The angle between the incident and reflected beams then formed a 90° angle as shown in figure 2(*b*).

The dimensions of the LDA measuring volume were $0.053\,\text{mm} \times 0.053\,\text{mm} \times 0.77\,\text{mm}$ (or $0.5 \times 0.5 \times 7$ in wall units based on the lowest flow rate) with the longest dimension being in the x-direction, as specified in figure 2. It was moved along the x-axis to make measurements of the axial and circumferential velocity components (u and w) and moved along the y-axis to make measurements of the axial and radial velocity components (u and v). The fact that such measurements are made over a volume of finite dimension and that the velocity gradient increases near the wall can lead to error. In the present investigation, the error in the evaluation of turbulence stresses associated with such reasons was estimated using the formula due to Durst *et al.* (1994) to be less than 10%.

The experimental uncertainties in mean velocity measurement in the present experiments were mainly due to (*a*) limitations in the repeatability of flow control and accuracy of flow measurement, (*b*) uncertainty in determining the LDA frequency–velocity coefficient and (*c*) the accuracy of the frequency tracker. The combined uncertainty was estimated to be less than 10%. The uncertainties in the measurements of turbulence quantities were mainly due to the limitations of the trackers. In the region near the wall, error could also result from inaccuracy in position control and the averaging over the finite dimension of the measuring volume. The maximum uncertainty in the measured turbulence quantities was estimated to be about 20%. Very near the wall, 'drop-out' of the tracker signal sometimes occurred due to poor quality of signal, caused perhaps by the presence of dirt on the surface of the test section. This increased the uncertainty of some of the measurements.

Some measurements of turbulent stresses made in the present study under con-

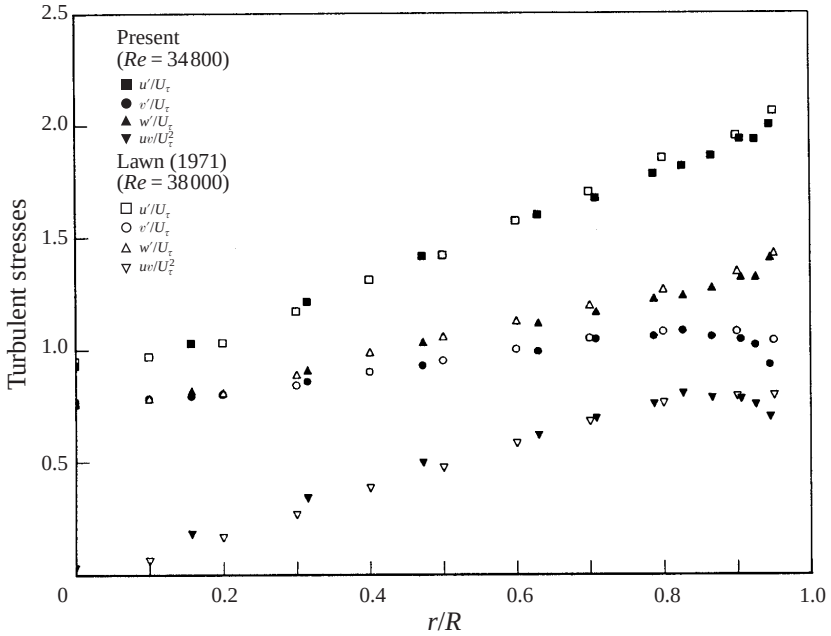

FIGURE 3. Turbulent stresses in a fully developed pipe flow.

ditions of steady flow at a Reynolds number of 34 800 are presented in figure 3. Also shown are measurements made using hot-wire probes in a detailed study of fully developed pipe flow reported by Lawn (1971). These were chosen for comparison with the present data because of the very careful attention paid to the accuracy in that study, and also because of the close match in terms of Reynolds number. It can be seen from the figure that the two sets of measurements are in good agreement. The measurements of normalized turbulent shear stress from both studies follow closely the linear variation expected for fully developed pipe flow over the region where turbulent shear stress dominates viscous shear stress.

2.3. *Flow control and data acquisition systems*

The flow control and data acquisition system shown in figure 1 was developed specially for use in this study. It utilized two personal computers and a Microvax system. PCI modules were used for interfacing the computers with the experiment. These made digital to analogue and analogue to digital conversions and incorporated standard clock, trigger signal and other special functions.

Flow control was achieved using one of the personal computers in conjunction with an electronic position controller and a pneumatic activator. A prescribed flow rate was converted to a valve-opening signal in the computer and sent to the electronic position controller. The latter then drove the pneumatic activator to operate the valve until the demanded opening had been achieved. Very accurate flow control with excellent repeatability was achieved using this system. The flow rate passing through the test section was measured by the turbine flow meter, the electrical output signal from which was of square-wave form with a frequency proportional to flow rate. The frequency of the signal was determined using the computer which performed the flow control to measure the time interval of the square wave using the standard clock.

Two data sampling schemes were available. In the case of the first one, up to eight

channels of data could be sampled at high speed (utilizing a personal computer and the Microvax). The data collected were sent directly to the Microvax which had a large memory for data storage and performed data processing at high speed. In the second scheme, data could be sampled using a personal computer with the use of the sample-and-hold technique to ensure that information sampled from different channels corresponded to exactly the same point in time. This was necessary for correlation calculations. The highest possible sample rate with this arrangement was approximately 15 kHz. Approximately 540 kbytes of the dynamic memory of the computer were made available to serve as the data buffer. This was enough for most of the experiments carried out except for the two longest tests (excursions of flow rate over time periods of 45 and 90 s). The sample rate for these tests was reduced in order to make continuous sampling possible.

2.4. *Data processing*

For a ramp-type excursion of flow rate, the instantaneous local velocity can be decomposed into an ensemble-averaged mean velocity and a turbulent fluctuating velocity. The ensemble-averaged mean velocity U is defined as

$$U(t) = \lim_{N\to\infty} \frac{1}{N} \sum_{i=1}^{N} u_i(t), \tag{3}$$

where u_i represents any component of the instantaneous velocity of the ith repeat of the flow transient, t is the time which has elapsed after the start of the transient and N is the total number the flow excursion repeats, which in practice has to be a large number. The ensemble-averaged normal stresses are defined as

$$\overline{u(t)^2} = \lim_{N\to\infty} \frac{1}{N} \sum_{i=1}^{N} [u_i(t) - U(t)]^2, \tag{4}$$

$$\overline{v(t)^2} = \lim_{N\to\infty} \frac{1}{N} \sum_{i=1}^{N} v_i(t)^2, \tag{5}$$

$$\overline{w(t)^2} = \lim_{N\to\infty} \frac{1}{N} \sum_{i=1}^{N} w_i(t)^2, \tag{6}$$

and the ensemble-averaged shear stress as

$$\overline{uv(t)} = \lim_{N\to\infty} \frac{1}{N} \sum_{i=1}^{N} [u_i(t) - U(t)] v_i(t). \tag{7}$$

The root-mean-square values of components of turbulent velocity fluctuations are then defined under the concept of ensemble averaging as

$$u'(t) = \sqrt{\overline{u(t)^2}}, \quad v'(t) = \sqrt{\overline{v(t)^2}}, \quad w'(t) = \sqrt{\overline{w(t)^2}}. \tag{8}$$

It should be noted that rather than utilizing the brackets notation $\langle\ \rangle$, capital characters or small characters with a bar above them will be used to denote ensemble-averaged values. The term 'mean' will be used to denote the ensemble average unless otherwise stated.

It was found from preliminary experiments that at least several hundred samples were needed before convergence was achieved in the calculation of local mean velocity

and turbulence quantities. Obviously, it was not a practical proposition to perform many hundreds of experimental realizations to obtain ensemble-averaged information for the ramp-type flow excursions studied in this investigation. For example, up to 10 hours would have been needed to make 600 runs for experiments at a single location in the case of an excursion of time period 20 s. Even if one could have afforded the time, variations in the experimental conditions over a 10 hour time period would have posed a problem. A modified ensemble-averaging scheme was therefore employed in the present investigation in order to reduce the number of realizations needed. With this modified scheme, the duration of a transient is divided into a number of small windows, each of which contains a number of samples. The number of windows was chosen so that the variation of the mean velocity in each of the windows was much less than the turbulent fluctuating velocity during the same period. The ensemble-averaged mean velocity within each window was therefore taken to be constant and the conventional ensemble-average procedure was applied to each window rather than each point for the purpose of computing mean velocity and root-mean-square fluctuation of velocity.

Under the modified scheme, the ensemble-averaged mean velocity can be expressed as

$$U_k = \frac{1}{NM} \sum_{i=1}^{N} \sum_{j=1}^{M} u_{i,j+(k-1)M} \tag{9}$$

and the Reynolds stresses expressed as

$$\overline{u_k^2} = \frac{1}{NM} \sum_{i=1}^{N} \sum_{j=1}^{M} (u_{i,j+(k-1)M} - U_k)^2, \tag{10}$$

$$\overline{v_k^2} = \frac{1}{NM} \sum_{i=1}^{N} \sum_{j=1}^{M} v_{i,j+(k-1)M}^2, \tag{11}$$

$$\overline{w_k^2} = \frac{1}{NM} \sum_{i=1}^{N} \sum_{j=1}^{M} w_{i,j+(k-1)M}^2, \tag{12}$$

$$\overline{uv_k} = \frac{1}{NM} \sum_{i=1}^{N} \sum_{j=1}^{M} (u_{i,j+(k-1)M} - U_k) v_{i,j+(k-1)M}, \tag{13}$$

where $k = 1, 2, \ldots, L$ and L is the number of windows in a realization of the transient. M and N denote the number of samples in each window and the number of repeats of the transient respectively; $u_{i,j+(k-1)M}$, is the $(j+(k-1)M)$th sample of the instantaneous velocity for the ith run.

2.5. *Experimental conditions*

In the main experimental program of the present study, ramp-up experiments were performed in which the ramp rate $\mathrm{d}U_b/\mathrm{d}t$ was varied by imposing excursions of flow rate during which the bulk velocity increased linearly with time from an initial value U_{b0} of $0.138\,\mathrm{m\,s^{-1}}$ to a final value U_{b1} of $0.891\,\mathrm{m\,s^{-1}}$ in periods of time which ranged from 2 s to 90 s. Thus, the initial and final Reynolds numbers Re_0 and Re_1 were constant (at the values 7000 and 45 200) but the dimensionless ramp rate parameter γ increased systematically from 0.34 (pseudo-steady flow) to 15.3 (unsteady turbulent flow). Corresponding experiments were performed in which ramp-down

	No.	Initial Reynolds number	Final Reynolds number	Time period (s)	$dU/Dt\,(m\,s^{-2})$	$\gamma\left(=\frac{dU_b}{dt}\frac{1}{U_{b0}}\frac{D}{U_{\tau 0}}\right)$
(*a*)	1	7000	45200	2	0.378	15.3
	2	7000	45200	5	0.151	6.1
	3	7000	45200	10	0.0754	3.1
	4	7000	45200	15	0.0503	2.0
	5	7000	45200	25	0.0302	1.2
	6	7000	45200	45	0.0168	0.68
	7	7000	45200	90	0.0084	0.34
	8	13900	45200	8.2	0.0754	0.81
	9	20900	45200	6.36	0.0754	0.39
	10	27800	45200	4.55	0.0754	0.23
(*b*)	1	45200	7000	2	−0.378	−0.46
	2	45200	7000	5	−0.151	−0.19
	3	45200	7000	10	−0.0754	−0.093
	4	45200	7000	15	−0.0503	−0.062
	5	45200	7000	25	−0.0302	−0.037
	6	45200	7000	45	−0.0168	−0.021
	7	34800	7000	7.27	−0.0754	−0.15
	8	27800	7000	5.45	−0.0754	−0.23
	9	20900	7000	3.64	−0.0754	−0.39

TABLE 1. Experimental conditions: (*a*) ramp-up excursions, (*b*) ramp-down excursions. The ramp rate parameter γ was calculated based on the starting flow conditions. For a ramp-up transient, this parameter decreases as the flow increases. For a ramp-down transient, it increases as the flow decreases. In this case, delays can be significantly larger in the later stages of the excursion than the values shown in the table might suggest.

excursions of flow rate were imposed. Bulk velocity decreased from $0.891\,m\,s^{-1}$ to $0.138\,m\,s^{-1}$ over periods of time which ranged from 45 s to 2 s. Thus, the initial and final Reynolds numbers Re_0 were constant (at the values 45 200 and 7000) and the dimensionless ramp rate parameter γ varied systematically in the range −0.021 to −0.46. It should be noted that the above values of γ are based on the parameters at the start of the excursions and should not therefore be taken as suggesting that the conditions of pseudo-steady flow prevailed throughout. As a ramp-down excursion of flow rate proceeds, the velocity and time scales reduce and delays in the response of turbulence become progressively longer. Therefore, greater departures from pseudo-steady conditions develop.

In a further programme of experiments, ramp-up and ramp-down excursions were imposed in which the initial velocity was varied but the ramp rate was kept fixed. In those experiments, both the initial Reynolds number Re_0 and the dimensionless ramp rate parameter γ varied but the final Reynolds number Re_1 was constant. In the ramp-up experiments, the parameters Re_0 and γ were respectively 7000 and 3.1, 13 900 and 0.81, 20 900 and 0.39, 27 800 and 0.23 and Re_1 was 45 200. Thus the conditions varied from those of unsteady turbulent pipe flow to pseudo-steady flow. In the corresponding ramp-down experiments Re_0 and γ were respectively 45 200 and −0.093, 34 800 and −0.15, 27 800 and −0.23, 20 900 and −0.39 and the final Reynolds number Re_1 was 7000.

The experimental conditions covered in the present investigation are summarized in table 1. The locations where velocity measurements were made are shown in table

No.	r (mm)	r/R	y (mm)	y_0^{+*}	y_1^{+**}
1	0	0.0	25.4	228.6	1168
2	4	0.157	21.4	192.6	984.4
3	8	0.315	17.4	156.6	800.4
4	12	0.472	13.4	120.6	616.4
5	16	0.63	9.4	84.6	432.4
6	18	0.71	7.4	66.6	340.4
7	20	0.787	5.4	48.6	248.4
8	21	0.827	4.4	39.6	202.4
9	22	0.866	3.4	30.6	156.4
10	23	0.906	2.4	21.6	110.4
11	23.5	0.925	1.9	17.1	87.4
12	24	0.945	1.4	12.6	64.4

TABLE 2. Measurement locations. $y_0^{+*} = yU_\tau/\nu$, in which $U_\tau = 0.009$ for Reynolds number 7000 (start of flow transient) and $\nu = 10^{-6}\mathrm{m}^2/\mathrm{s}^{-1}$; $y_1^{+**} = yU_\tau/\nu$, in which $U_\tau = 0.046$ for Reynolds number 45 200 (end of flow transient) and $\nu = 10^{-6}\mathrm{m}^2\,\mathrm{s}^{-1}$.

2. Also shown in that table are distances from the wall, non-dimensionalized using viscous lengths corresponding to the starting and end flow rates, respectively.

In addition to the transient flow experiments, a series of steady-state experiments were performed at a number of particular flow rates within the range covered in the transient flow experiments. The data obtained were time averaged in the usual manner for steady flow to give mean velocity and turbulence quantities. The results provide a pseudo-steady-state reference for comparison with data obtained in the transient flow experiments.

3. Experimental results

3.1. *Ensemble-averaged local mean velocity*

The development of local mean velocity throughout a 5 s time period ramp-up excursion of flow rate ($Re_0 = 7000$ and $\gamma = 6.1$) of the main experimental programme is shown in figure 4 for a number of radial positions. The results are plotted as a function of Reynolds number but since this is directly related to flow rate, the increase of which is proportional to the time from the start of the excursion, the variation is the same as it would be with time.

A clear difference can be seen in the response of the local velocity in core and wall regions. In the first part of the excursion, the rate of the increase of velocity tends to be similar at all positions. When compared with pseudo-steady flow variations, the flow in the near-wall region over-responds and that in the core region under-responds. This trend is reversed during the excursion. The same set of data is re-plotted in figure 5 in the form of profiles of local mean velocity at a number of stages in the excursion. These are shown together with the corresponding measured pseudo-steady-state velocity profiles. It can be clearly seen that in the early stage of the transient the velocity profile is flattened, an effect which has also been found in the acceleration stage of pulsating flows (Tu & Ramaprian 1983). Later, the profile approaches the pseudo-steady shape. There is almost no distortion of the profile towards the end of the excursion.

The features just identified of the response of the local mean velocity for the 5 s time period ramp-up flow excursion were also evident in corresponding ramp-up results

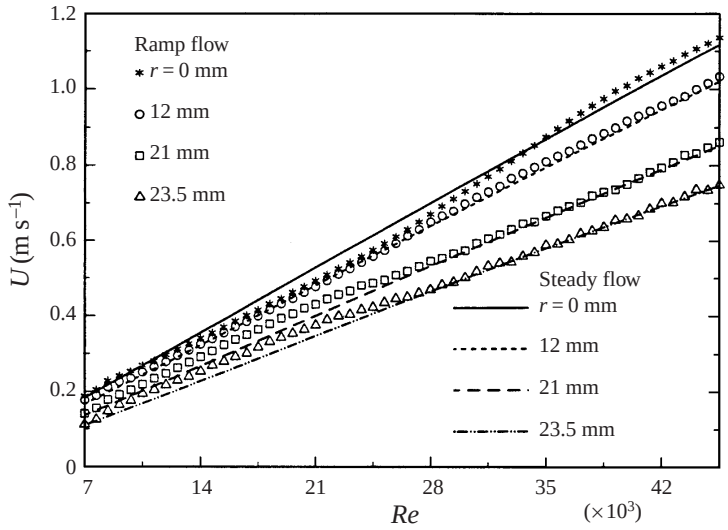

FIGURE 4. Variation of local mean velocity in a 5 s time period ramp-up flow excursion.

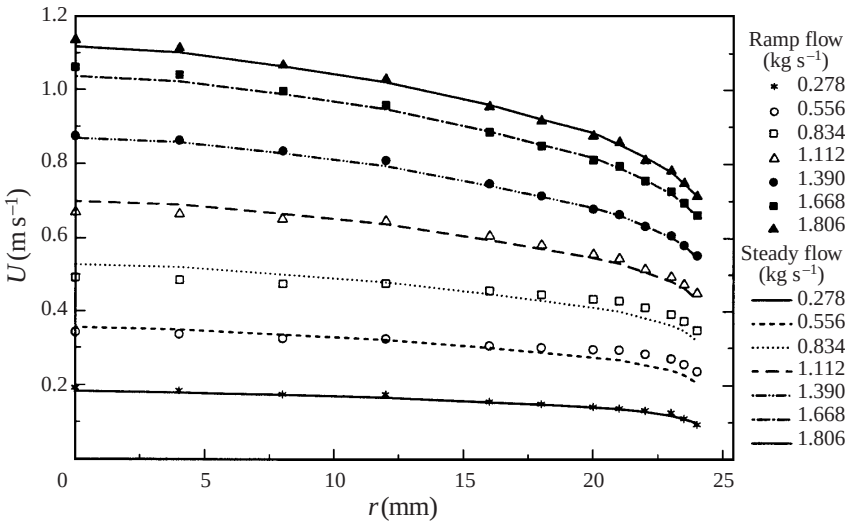

FIGURE 5. Development of local mean velocity profile in a 5 s time period ramp-up flow excursion.

for time periods of 10 and 15 s (not presented here) for which $\gamma = 3.1$ and 2.0. The departures of the profiles from the corresponding pseudo-steady shapes are smaller than in the case of the 5 s time period case and they are limited to earlier stages of the excursion. However, in terms of absolute time from the start of a transient, the distortion of the velocity distribution occurs over approximately the same period. Figure 6 shows results for a ramp-up excursion of flow rate with a time period of 45 s, for which $\gamma = 0.68$. It is clear that for this case the local mean velocity is virtually identical to that for pseudo-steady flow.

3.2. *Turbulence field*

The time variation of the axial component of RMS velocity fluctuation during a 5 s time period ramp-up flow excursion (with $\gamma = 6.1$) is shown in figure 7 for

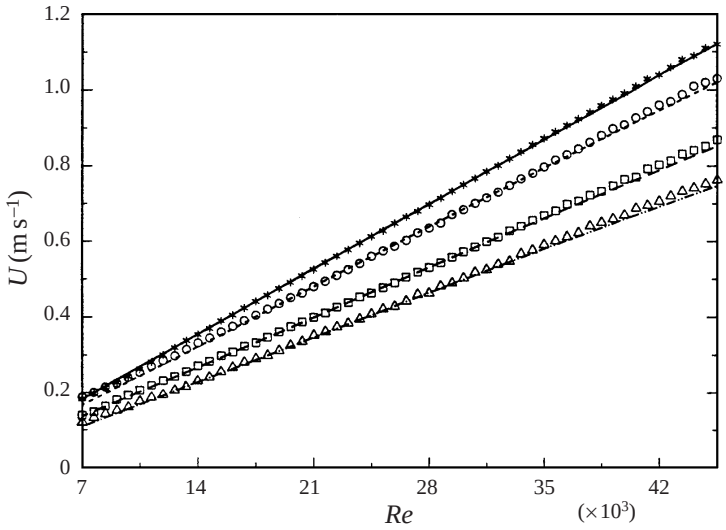

FIGURE 6. Variation of local mean velocity in a 45 s time period ramp-up flow excursion. Symbols as in figure 4.

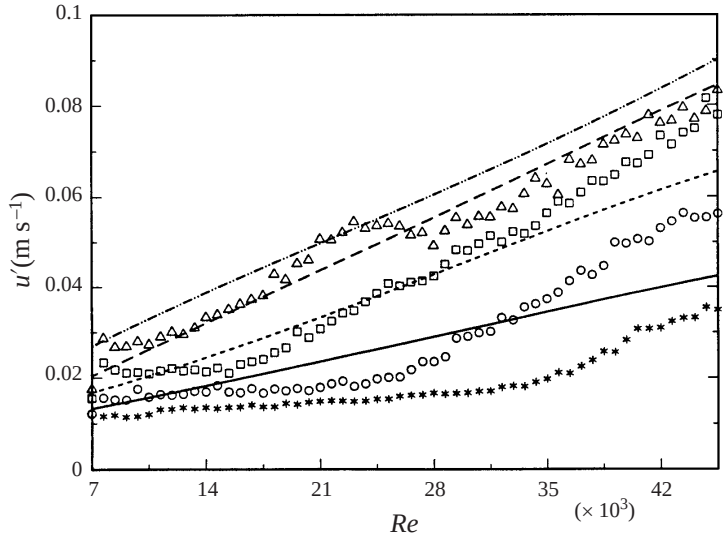

FIGURE 7. Variation of RMS fluctuation of axial velocity component in a 5 s time period ramp-up flow excursion. Symbols as in figure 4.

several radial positions. The corresponding pseudo-steady results are also shown for comparison. One of the most striking features of the response of velocity fluctuation to the imposed flow transient is a 'delay' effect. As can be seen, the turbulent velocity fluctuation u' does not follow the corresponding pseudo-steady variation, but instead exhibits a two-stage variation. In the core region, there is a very slow response for much of the excursion period after which a marked change occurs and u' builds up at a much faster rate. The discrepancies between the transient values and the pseudo-steady values reduce during the later period of the excursion but the transient values are still well below the steady-state values even at the end of the excursion.

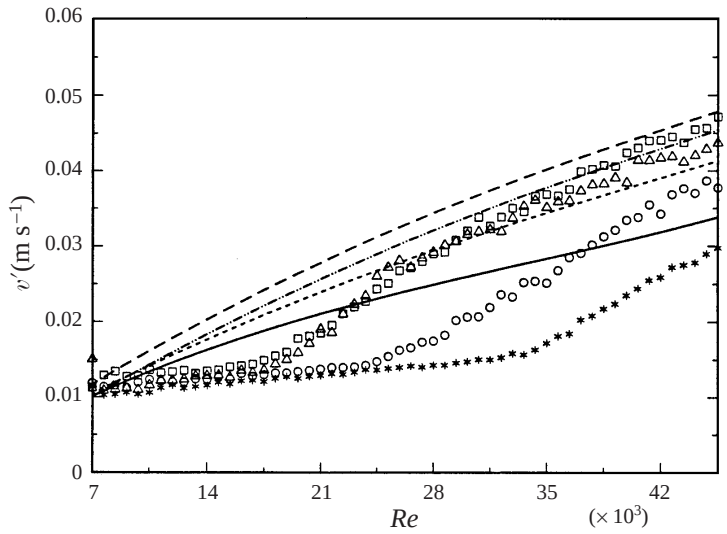

FIGURE 8. Variation of RMS fluctuation of radial velocity component in a 5 s time period ramp-up flow excursion. Symbols as in figure 4.

Very close to the wall, the behaviour is more complicated. There, an additional feature is evident. A rapid upsurge in u' to the steady-state value occurs after a very slight initial delay. Then there is a slight fall followed by a recovery.

The period of time from the start of an excursion to the point at which the faster response starts will be described here as the delay period τ. This is clearly a function of radial position. Very near the wall the delay is less than 1 s. The further the position is away from the wall, the longer is the delay. At the centre it approaches 4 s. Within the core, the magnitude of the u' does not remain absolutely unchanged during the delay period but rather increases slowly. The rate of increase remains constant throughout the delay and appears to be the same at various positions.

It can be seen that the response of u' to the imposed excursion starts in the wall region and is transmitted at a certain speed towards the centre of the pipe. We will see later (§ 4.3) that this is related to the friction velocity $U_{\tau 0}$ at the start of the excursion. These observations can be related to those made by Shemer *et al.* (1985) and Tardu *et al.* (1994) for pulsating flows, in which the phase shift of the response of turbulence quantities was found to increase with distance from the wall. Clearly, both effects result from delays associated with the propagation of the response of turbulence. Similarly, in the study of unsteady pipe flow with stepwise increases of flow rate of Maruyama *et al.* (1976) a delay in the radial propagation of the response of turbulence was also clearly evident.

The development of the radial and circumferential components of the RMS turbulent fluctuation velocity v' and w' is shown in figures 8 and 9, respectively, for the 5 s time period ramp-up case. Some of the features of the response of u' described above can also be seen in the response of v' and w'. The most striking feature is again a two-stage development. After the onset of the excursion of flow rate, the v' and w' components do not follow the pseudo-steady variation. Instead, they both exhibit delayed responses for a period of time during which their variation is slight. The delays increase with increase of distance from the wall. However, near the wall in the region $r/R \geqslant 0.79$ (for which $y^+ \leqslant 50$) the responses of v' and w' are different

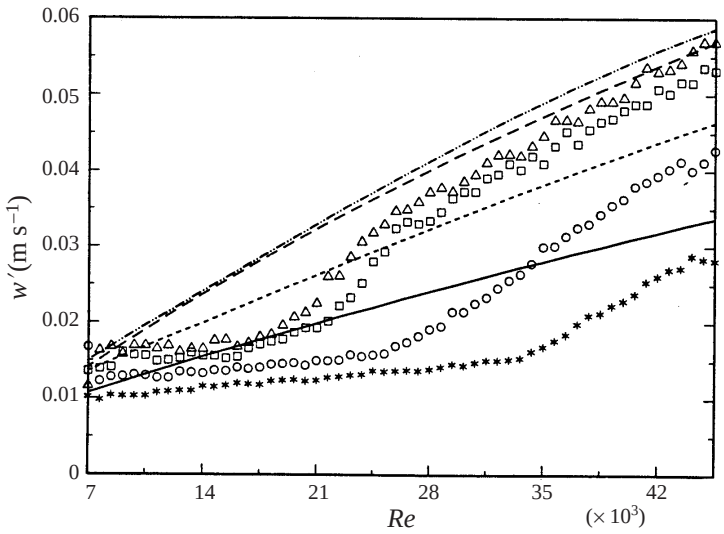

FIGURE 9. Variation of RMS fluctuation of circumferential velocity component in a 5 s time period ramp-up flow excursion. Symbols as in figure 4.

from that of u'. Instead of responding to the imposed transient after a very short delay (a fraction of a second), the first stage of the response lasts for over a second and does not depend on distance from the wall. The upsurge seen in the case of u' is not found. The different behaviour stems from the mechanisms in the supply of energy to the various components. The axial component of turbulent energy is directly extracted from the mean flow through the shear stress and the velocity gradient. The change of the velocity profile under the action of the additional pressure gradient initially results in direct generation of additional turbulent motion in the axial direction. The main source of the increased radial and circumferential components of the turbulent energy which develop later comes from the redistribution from the axial direction through pressure strain. The time difference between the initial response of u' and those of v' and w' provides an indication of the time scale for such processes.

The development of the axial and radial components of turbulence in the 5 s time period ramp-up excursion are re-plotted in figure 10 with the fluctuations normalized using the ensemble-averaged bulk velocity (i.e. as turbulence intensities). It can be seen that turbulence intensity is attenuated in accelerating transient flow. This is clearly consistent with the well-established behaviour in flows under spatial acceleration, see for example, Narayanan & Ramjee (1969), Blackwelder & Kovasznay (1972), Baskaran *et al.* (1987) and Webster *et al.* (1996) for boundary layer flows subjected to favourable pressure gradients and Tanaka & Yabuki (1986), Sano & Asako (1993) and Spencer *et al.* (1993) for internal flows in contractions. However, as can be seen from figures 7 and 8, the absolute values of u' and v' do not actually reduce. The reduction in turbulence intensity is a consequence of the delayed response of the turbulence quantities. As the ensemble-averaged mean velocity increases, u' and v' remain at or near to their initial values or increase at a rate slower than their pseudo-steady counterparts. Blackwelder & Kovasznay (1972) and Tanaka & Yabuki (1986) both pointed out in their studies (of relaminarization in a boundary layer flow and a converging channel flow respectively) that the absolute value of turbulence stresses

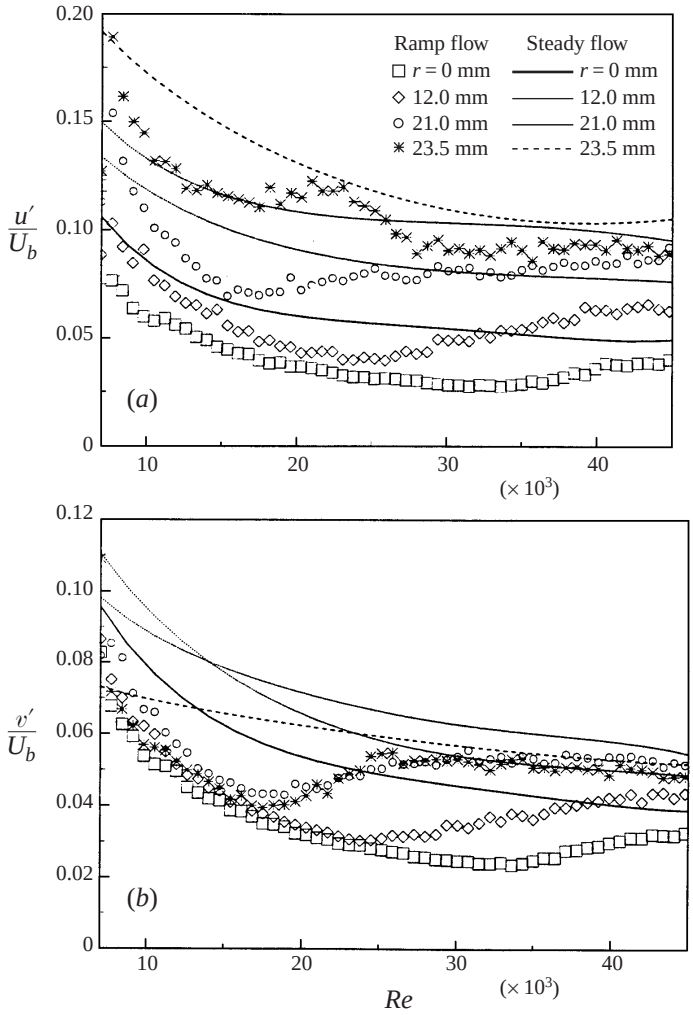

FIGURE 10. Variation of turbulence intensity in a 5 s time period ramp-up flow excursion. (*a*) Axial component, (*b*) radial component.

did not reduce, although the intensity reduced significantly. The reason they gave was that the acceleration was relatively mild.

The time development of ensemble-averaged turbulent shear stress in the 5 s time period ramp-up flow excursion is shown in figure 11 for a number of radial positions. This response also exhibits the features of delay and propagation. After the imposition of the excursion, turbulent shear stress remains completely unchanged for a period. There then follows a stage during which it builds up towards the pseudo-steady flow value. As in the case of the normal stresses and also the turbulent kinetic energy, the delay at positions in the core region is dependent on the distance from the wall. In the wall region the development of the turbulent shear stress is similar to that of the radial and circumferential components of the turbulence, exhibiting a distinct delay for a period which is independent of the location. The main difference between the response of the shear stress and the normal stresses is that shear stress remains virtually unchanged during the delay period whereas the normal stresses (and the

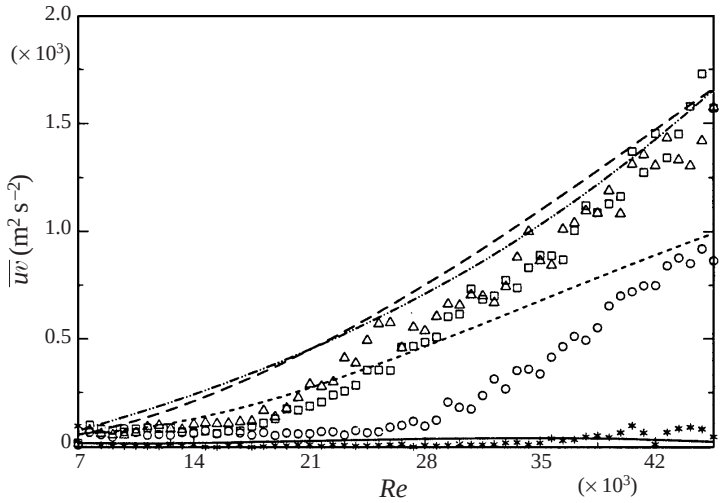

FIGURE 11. Variation of turbulent shear stress in a 5 s time period ramp-up flow excursion. Symbols as in figure 4.

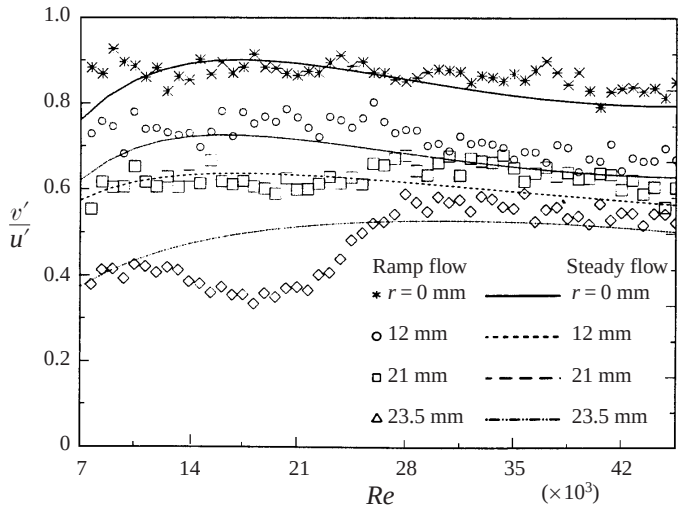

FIGURE 12. Variation of the ratio of v'/u' in a 5 s time period ramp-up flow excursion.

turbulent kinetic energy) increase slowly during this period, although the increases are small compared with the corresponding ones for pseudo-steady flow.

Figure 12 shows the development of the ratio of the radial to axial components of the turbulent velocity fluctuation at several radial positions across the section of the pipe during the 5 s time period ramp-up flow excursion. It is interesting to note that, in the core flow, the variation of this ratio generally follows that of pseudo-steady flow. A two-stage development is not manifested. This indicates that the mechanisms controlling the delay and recovery of turbulence in response to an imposed transient are quantitatively similar in that region for these two components. Webster *et al.* (1996) found a similar result. In their study of the turbulence characteristics of a boundary layer flow over a two-dimensional bump the normal stresses responded nearly identically. In contrast to the core region, the behaviour near the wall region

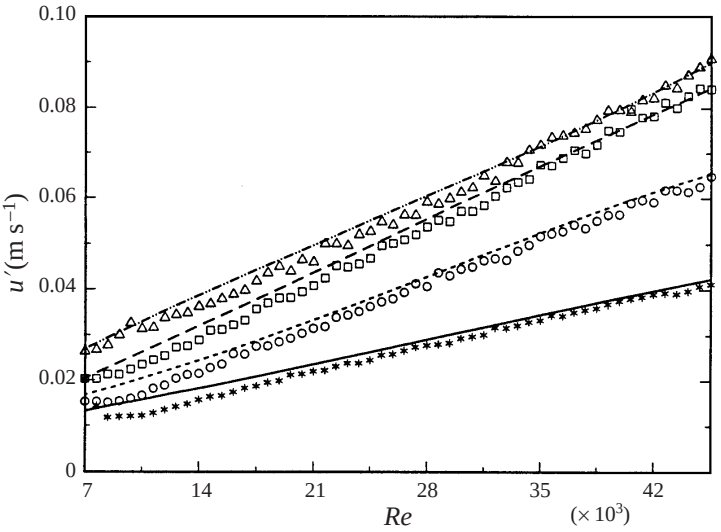

FIGURE 13. Variation of RMS fluctuation of axial velocity component in a 45 s time period ramp-up flow excursion. Symbols as in figure 4.

($r = 23.5$ m, $y^+ = 17$) is very different. After a very short delay, the ratio of v' to u' at first falls well below the pseudo-steady flow variation and remains at a low level for a period of approximately 1.8 s, after which it increases rapidly. Within a very short time, it reaches a level which is slightly higher than the pseudo-steady flow counterpart and remains so until the end of the imposed flow excursion. The periods of time for the reduction and for the recovery are the same for all radial positions in the near-wall region. The extent of the reduction is different though. This behaviour can be associated with the way energy is supplied to the various components. Whereas the axial component of turbulent energy is directly extracted from the mean flow through the shear stress and the velocity gradient, the main source of additional radial and circumferential components of the turbulent energy stems from the redistribution from the axial component through pressure strain.

We next consider the response of turbulence in a very slow transient (the 45 s time period ramp-up flow excursion, for which $Re_0 = 7000$ and $\gamma = 0.68$). From figure 13, it can be seen that delays in the response of u' in the early stages of flow excursion are still evident even in such a slow transient, again reaching a value of about 4 s in the core, although as seen earlier the mean velocity distributions are in close agreement with the corresponding pseudo-steady-state ones. In the later stages, however, u' does not deviate much from the corresponding values for pseudo-steady flow.

On examining the responses of the u' turbulent fluctuation in the core flow to ramp-up excursions of flow rate of various time periods from 5 to 45 s, one finds that the delays are in all cases more or less the same at a particular position despite the imposed acceleration being very different. A comparison of the responses of turbulence at the centre of the pipe for ramp-up excursions of various time period is shown in figure 14. The change-over points of the response curves are indicated with arrows. The absolute delays are given in table 3. It is apparent that they deviate little from a mean value of about 4 s, so that there is no systematic effect of the imposed flow acceleration on the delay. However, as can be seen from figure 14, the deviations of the u' responses for transient flow from the corresponding pseudo-

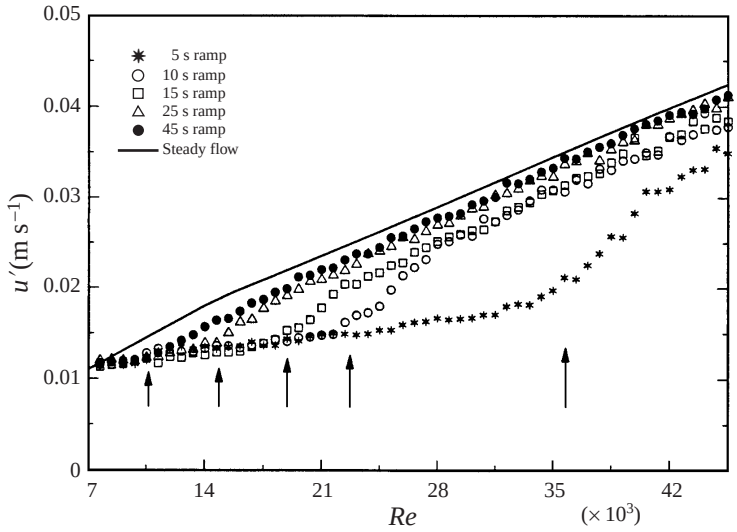

FIGURE 14. Comparison of the responses of RMS fluctuation of axial velocity component at pipe centre for various ramp rates.

Ramp time period (s)	5	10	15	25	45
Dimensionless ramp rate parameter γ	6.1	3.1	2	1.5	0.68
Delay τ (s)	3.9	4.1	4.0	3.9	4.0

TABLE 3. Absolute delays at the centre of the pipe.

steady variations differ significantly. They decrease progressively with reduction of ramp rate parameter. However, even for the 45 s time period excursion ($\gamma = 0.68$), some deviation is evident.

The corresponding variations of the radial component of the turbulent fluctuation velocity v' at the centre of the pipe for ramp-up excursions of flow rate of various time periods are plotted in figure 15. It is clear that the behaviour is very similar to that of u'. The time scales for the response of the two components are practically the same at the centre of the pipe. There is no evidence of energy transfer from the axial component to the radial one in this region. In other words, the time scales associated with pressure–strain effects are negligible compared with those for turbulence diffusion in the core region. Shemer *et al.* (1985) arrived at the same conclusion after examining the responses of u' and v' in a pulsating flow.

Figures 16 and 17 show the development of u' and v' in a 5 s time period ramp-down transient flow (for which $\gamma = -0.19$) along with the corresponding pseudo-steady variations. The spread of the data is greater than that in the corresponding cases for ramp-up flow. However, some interesting effects can still be seen. There is evidence of a delayed response which builds up with distance from the wall. However, the delay is much smaller than in the corresponding ramp-up excursion, only reaching a maximum of just under 1 s in the core region. During the subsequent fall, the transient values lie above the corresponding pseudo-steady values and the difference builds up slightly as the excursion proceeds. It is clear that the intensity of turbulence

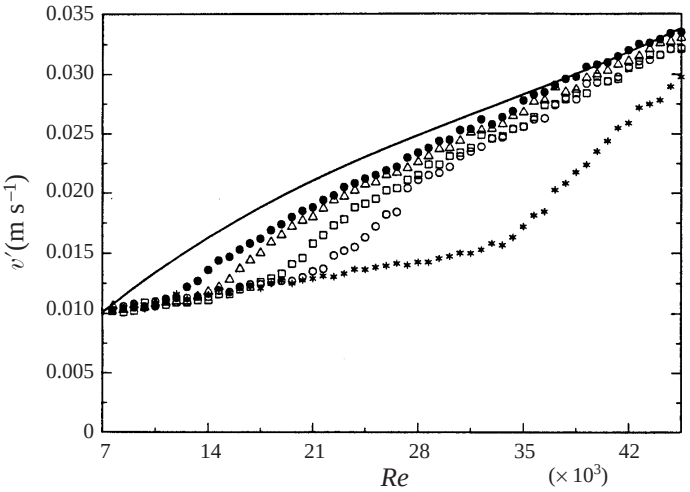

FIGURE 15. Comparison of the responses of RMS fluctuation of radial velocity component at the pipe centre for various ramp rates. Symbols are as in figure 14.

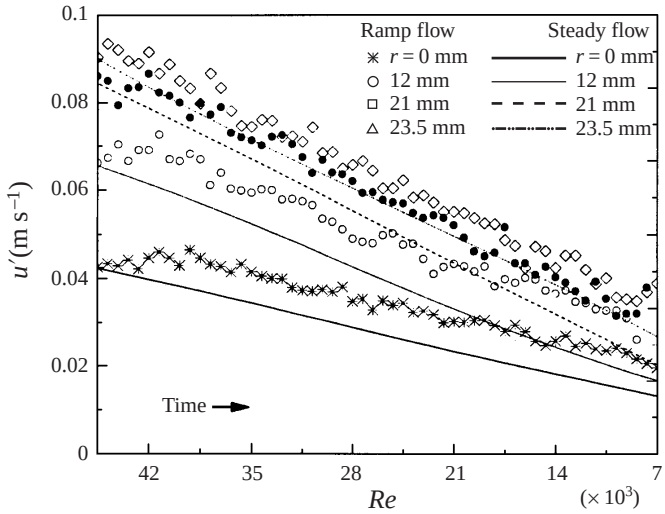

FIGURE 16. Variation of RMS fluctuation of axial velocity component in a 5 s time period ramp-down flow excursion.

is greater in the transient flow case than for steady flow. The features exhibited by these ramp-down experiments will be considered further later in the paper.

We next consider the further programme of experiments which was conducted with a view to studying the effect of the starting flow rate of the imposed excursions on the response of turbulence. In the case of ramp-up excursions the starting flow rate was varied systematically between 0.278 to 1.11 kg s^{-1} (corresponding to values of Reynolds number of 7000 and 27 800). By adjusting the time period for each experiment, the ramp rate $\mathrm{d}U_b/\mathrm{d}t$ was kept constant at the value equal to that for the 10 s ramp-up flow excursions of the main series of experiments discussed earlier. Ramp-down experiments, starting from various flow rates in the range 0.834 to 1.806 kg s^{-1} (corresponding to the values of Reynolds number of 20 900 and 45 200)

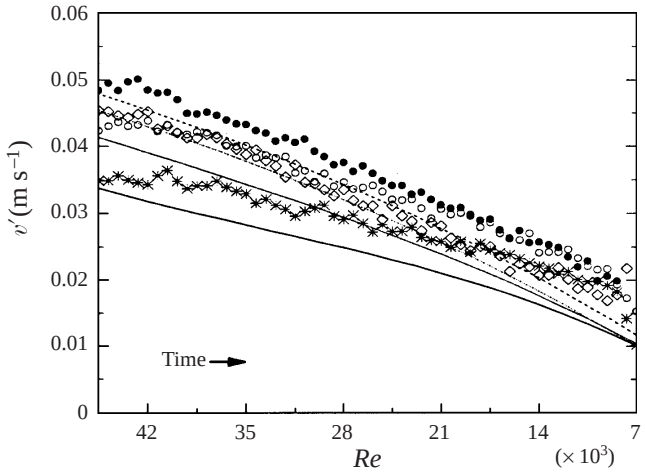

FIGURE 17. Variation of RMS fluctuation of radial velocity component in a 5 s time period ramp-down flow excursion. Symbols are as in figure 16.

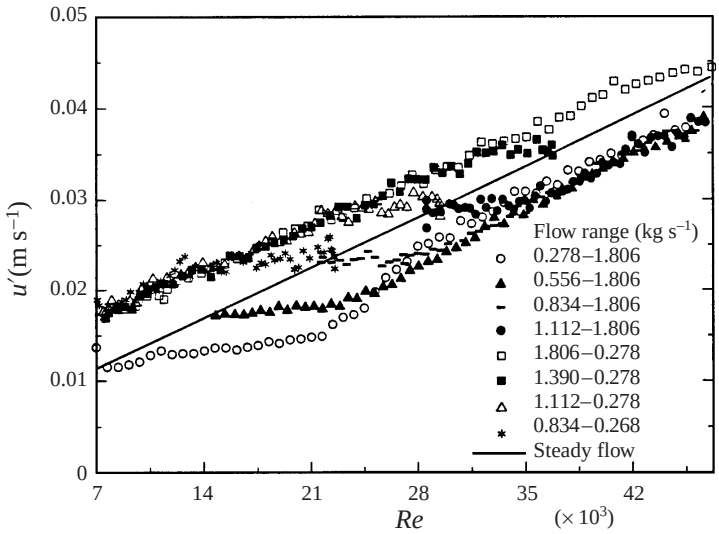

FIGURE 18. Influence of starting Reynolds number on the response at pipe centre of the RMS fluctuation of axial component for ramp-up and ramp-down excursion of flow rate.

and ending at a flow rate of 0.278 kg s^{-1} (Reynolds number 7000) were also performed. The time periods were again chosen to give a ramp rate of the same absolute value as that for the 10 s time period ramp-up experiment of the first series.

In this programme of experiments, measurements were only made at the centre of the pipe. The u' responses obtained are shown in figure 18, where the effect of varying the starting flow rate on the initial delay in the response of the turbulence can be clearly seen for both the ramp-up and ramp-down cases. With the increase of the starting flow rate, the delay systematically decreases. This appears to be so whether the imposed transient involves accelerating or decelerating the fluid. In the later stages of the excursions, all the data for the ramp-up experiments collapse onto a single line and those for the ramp-down tests all collapse onto another one. A similar picture

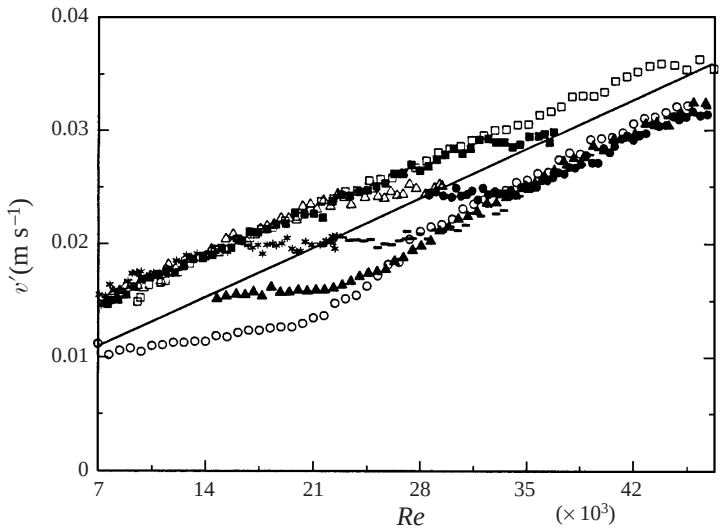

FIGURE 19. Influence of starting Reynolds number on the response at pipe centre of the RMS fluctuation of radial velocity component for ramp-up and ramp-down excursion of flow rate. Symbols are as in figure 18.

is provided by the results in figure 19, where the corresponding development of v' is presented.

4. Discussion of results

4.1. *Inertial effect*

Taking a time mean view of steady fully developed turbulent pipe flow, two forces can be thought of as acting on the fluid within a fixed elemental control volume and being in balance with each other. These are a net pressure force resulting from the applied gradient and a net shear force due to the combined action of molecular diffusion and turbulent mixing. In the case of unsteady flow, the inertia of the fluid within the control volume must be considered as well. Taking an ensemble-average view of the problem, the equation describing the balance takes the following form:

$$\frac{\partial U}{\partial t} = -\frac{1}{\rho}\frac{\mathrm{d}P}{\mathrm{d}x} + \frac{1}{r\rho}\frac{\partial}{\partial r}(r\tau) \tag{14}$$

in which

$$\tau = \mu\frac{\partial U}{\partial r} - \rho\overline{uv}. \tag{15}$$

In the above equations, P is manometric pressure, t is time, x and r are the axial and radial coordinates, respectively, ρ is density, μ is dynamic viscosity and $\rho\overline{uv}$ is turbulent shear stress. As the distribution of velocity, the local turbulent shear stress and the applied pressure gradient are all known from the measurements made in the present study, each of the terms in (14) can be evaluated. However, due to experimental uncertainties, bearing in mind that the calculation of some of those terms involves either the first or the second derivatives of the measured distributions, one cannot expect to achieve an exact balance. In practice, the imbalance becomes particularly apparent near to the wall. The turbulent shear force derived from the

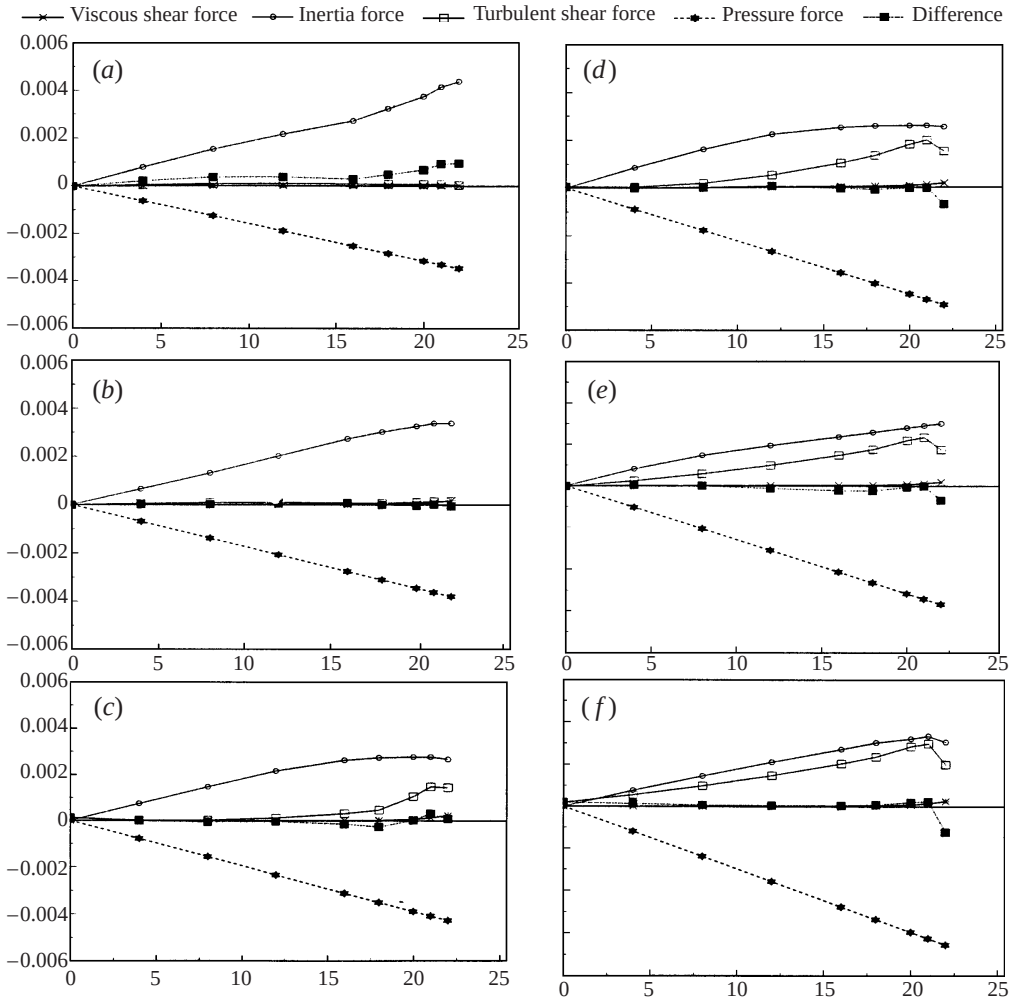

FIGURE 20. Comparison of momentum equation terms for 5 s time period ramp-up flow excursion (Inertia: $r(\partial u/\partial t)$, Pressure: $((r/\rho)(\mathrm{d}P)/(\mathrm{d}x))$, Viscous: $(-\partial/\partial r)[(rv)(\partial U/\partial r)]$, Turbulent: $(\partial/\partial r)[r\overline{uw}]$): (*a*) time = 0 s, flow rate = 0.278 kg s^{-1}, Re = 7000; (*b*) time = 0.91 s, flow rate = 0.556 kg s^{-1}, Re = 13 900; (*c*) time = 1.82 s, flow rate = 0.834 kg s^{-1}, Re = 20 900; (*d*) time = 2.73 s, flow rate = 1.112 kg s^{-1}, Re = 27 800; (*e*) time = 3.64 s, flow rate = 1.390 kg s^{-1}, Re = 34 800; (*f*) time = 4.55 s, flow rate = 1.668 kg s^{-1}, Re = 41 800.

derivatives of the measured turbulent shear stress presents particular difficulties and is not reliable for the region $r > 21$ mm.

The balances of the terms in (14) for $r \leqslant 21$ mm at a number of stages in the 5 and 45 s ramp-up flow excursion experiments (for which $Re_0 = 7000$ and $\gamma = 6.1$ and 0.68 respectively) are shown in figures 20 and 21. At an early stage in the 5 s time period excursion (0.91 s, figure 20*b*), the magnitudes of the pressure gradient force and the inertia force terms are much larger than the shear stress force terms and are approximately in balance with each another. As the excursion proceeds, the contribution of the turbulent shear force becomes progressively more and more significant (figures 20*c* onwards). The build-up of turbulent shear force starts in the wall region and gradually extends towards the centre. By the time the flow rate

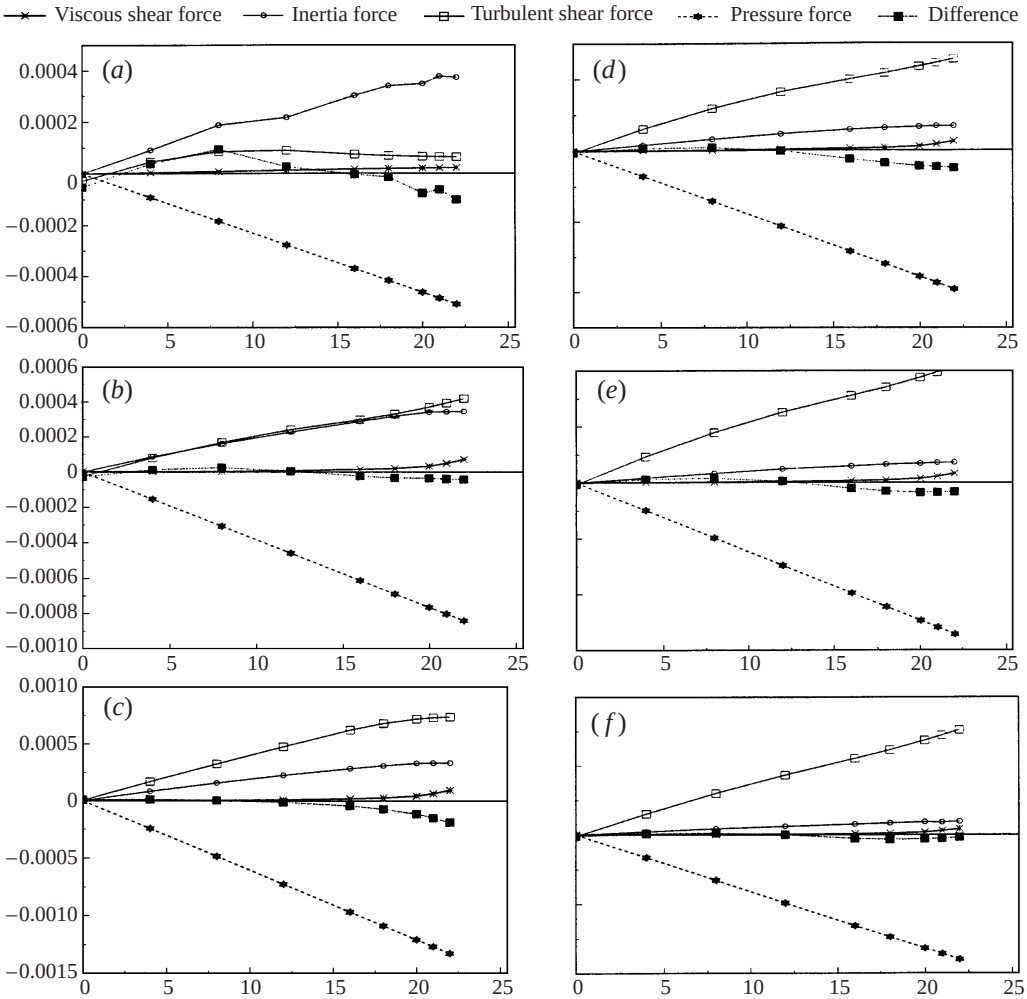

FIGURE 21. As figure 20 but for 45 s time period ramp-up flow excursion: (*a*) time = 0 s, flow rate = 0.278 kg s^{-1}, Re = 7000; (*b*) time = 8.2 s, flow rate = 0.556 kg s^{-1}, Re = 13 900; (*c*) time = 16.4 s, flow rate = 0.834 kg s^{-1}, Re = 20 900; (*d*) time = 24.6 s, flow rate = 1.112 kg s^{-1}, Re = 27 800; (*e*) time = 32.7 s, flow rate = 1.390 kg s^{-1}, Re = 34 800; (*f*) time = 40.9 s, flow rate = 1.668 kg s^{-1}, Re = 41 800.

reaches 1.39 kg s^{-1} (3.64 s, figure 20*e*), the distribution of the turbulent shear force between the wall region and the centre starts to approach the linear variation with radial position, characteristic of a fully developed steady flow. Even at this stage, however, the contribution of inertia to the balance is still greater than that of shear.

From figure 21, it can be seen that even for a very slowly rising ramp (45 s time period excursion, $\gamma = 0.68$), the contribution of inertia is still of importance in the early stages of the transient. Even a small acceleration involves an inertia force which makes a significant contribution to the balance. At the beginning of the excursion, the magnitudes of other terms in the momentum equation are relatively small. However, the turbulent shear force builds up rapidly and the inertia term becomes progressively smaller.

Although the contribution of inertia in the force balance is significant over a wide

range of conditions, its effect on the local mean velocity field is rather restricted. As we have seen earlier, a significant distortion of the mean velocity profile only occurs in the early stages of the faster transients. Under other conditions, the velocity profiles are similar to those of pseudo-steady flow even though the inertial contribution to the force balance is still significant.

An understanding of the effect of inertia on velocity profile shape during a ramp-up excursion can be arrived at as follows. In order to impose an excursion of flow rate, an extra pressure gradient is needed. In the very early stages of an excursion, the inertia force needed to accelerate the flow and the force due to viscous shear are in balance with the force due to the additional imposed pressure gradient as no additional turbulence exists. Since the distribution of the pressure gradient across the flow is uniform, the fluid tends to accelerate at a similar rate at all positions across the section. However, the fact that the velocity of the fluid must vanish at the wall acts as a constraint and consequently distortion of the profile must occur. At the beginning of the imposed transient, additional shear is confined to a very thin layer of fluid near to the wall. As a result, the velocity of the fluid in the core region initially responds to the additional pressure gradient almost as a 'slug'. The radial gradient of the velocity remains relatively unchanged in the core, but steep velocity gradients are generated in the wall region, to accommodate the increase in bulk velocity. Due to the combined influence of molecular diffusion and turbulent mixing, the effect of the wall constraint on the distribution of velocity propagates into the core region. This propagation occurs slowly in the viscous sublayer where molecular diffusion is the main mechanism for momentum transfer. However, this layer is thin. The propagation is faster in the region further out, where turbulent mixing becomes significant. Consequently, the wall constraint manifests itself more strongly in the viscous sublayer and more weakly in other regions. The degree to which the velocity profile is modified initially by the wall constraint is dependent on the thickness of the viscous sublayer (which is known to scale with $\nu/U_{\tau 0}$, where $U_{\tau 0}$ is the friction velocity at the start of the excursion), and this is determined by the initial Reynolds number. Propagation of the wall constraint has also been discussed in papers on pulsating flows. In that case, the Stokes sublayer $\sqrt{2\nu/\omega}$ is used. This provides a measure of the extent to which the wall constraint extends during a cycle of the flow variation (Mao & Hanratty 1986 and Tardu *et al.* 1994).

4.2. *Production and redistribution of turbulent energy*

As is well known, the energy of the turbulence field in a turbulent boundary layer is extracted from the organized mean flow. In simple shear flows, the production of turbulent kinetic energy occurs at a rate mainly determined by the product of the radial gradient of mean velocity and the turbulent shear stress. The response of the latter cannot precede that of turbulent kinetic energy, so the response of the turbulence field in transient flow initially results from changes of velocity gradient.

Upon imposing an extra pressure gradient to initiate a flow excursion, the velocity field starts to respond in the manner described in the preceding section. The increase of velocity gradient in the wall region offers a potential for increase in the production of turbulent energy but unless the region where the velocity gradient increases overlays that where turbulence production is high, i.e. the region within the buffer layer, the increase of the turbulence production will be confined to a low level. When the two regions do overlay each other, the production of turbulent energy will increase and an increase of turbulent kinetic energy will follow. We therefore expect to find a delay in the response of turbulence production in relation to the variation of the mean

flow. To form a time scale for this delay based on the physical picture, a length scale associated with the thickness of the buffer layer and a speed related to the molecular diffusion should be used. This leads to a time scale of the form ν/U_τ^2.

Delay in the response of turbulence production can be viewed differently utilizing the concept of turbulence bursting. Assuming that turbulence is produced locally in an intermittent manner as a result of turbulent bursts, production will not respond to an imposed variation of the flow until the next burst takes place. Some delay must therefore occur; the average value will be half the time interval between two bursts. This would again suggest that the delay in turbulence production might be scaled using the parameter ν/U_τ^2, which has been used to characterize the turbulence bursting frequency (Blackwelder & Haritonidis 1983).

Along with the build-up of turbulent energy in the buffer region, diffusion of turbulence to the adjacent areas increases and so does the turbulent energy in those areas. In the first instance, this is confined to the velocity component in the axial direction since the production of turbulence appears only in the conservation equation for that direction. Turbulent energy is later redistributed from the axial direction into other directions through the action of pressure strain. As mentioned earlier, it has been found from the present experimental results that as the axial component of turbulent energy increases the radial and circumferential components remain unchanged for a short period, after which both increase simultaneously over a region of flow near the wall. We can therefore speculate that turbulent disturbances in the axial direction, generated in the wall region, remain in this direction in the first instance during their transmission outwards into the core. On reaching a region further away from the wall, where the constraint of the wall is weaker, the axial flow disturbances break up and turbulent energy is re-arranged among the three directions. This action causes turbulent energy in the radial and circumferential directions to increase simultaneously over a relatively wide range of radial positions. Such energy redistribution has been noted by Baskaran *et al.* (1987) in an accelerating boundary layer in their study of turbulent flow over a curved hill. In that case, the redistribution of energy to the v' component was at the expense of the other two components.

4.3. *Turbulence propagation and the two-stage response*

It has been seen that an important feature of transient turbulent flow is that the response of the turbulence field starts first in a region very close to the wall and later propagates outwards into the core. The development of the turbulence quantities at any radial position can be divided into two stages. In the first stage, turbulence quantities remain unchanged or respond to the imposed transient at a rather slow rate. After a period of time (the delay), which is dependent on radial position and Reynolds number, additional turbulence originating from the wall region arrives at this position and a response of the turbulence quantities then follows at a much faster rate. However, these quantities are still smaller in the case of a rising ramp than the corresponding steady-state values and can be related to turbulence structure which existed sometime earlier in the wall region, i.e. at a time when flow rate was smaller. We will describe the two stages of the response as the 'delay stage' and the 'developing stage', respectively.

Assuming that the response of turbulence propagates as a result of turbulent diffusion at a characteristic velocity U_p and that the first response occurs at position y_0, the delay time at any position y can then be expressed as $(y - y_0)/U_p$. As seen earlier (figures 18 and 19), the delay in the response of the turbulence quantities depends on the starting Reynolds number. The greater the starting Reynolds number,

the shorter is the delay time and thus the greater is the propagation speed. A natural choice for the characteristic velocity of propagation in the turbulent region is the friction velocity U_τ, the velocity scale normally associated with turbulence diffusion. If we define a non-dimensional delay $\tau^+(=\sqrt{2}\tau U_{\tau 0}/D)$ using the time scale $R/U_{\tau 0}$ for turbulence diffusion over a distance R, we find that the observed delay at the centre of the pipe takes a constant value of about 1.0 for all the excursions considered so far. This serves to support the choice of U_τ as the characteristic velocity for turbulence propagation.

Utilizing the above ideas, we can now explain the observation made earlier in the case of the series of ramp-up experiments with the same initial Reynolds number that there was no influence of ramp rate on the delay in the response of turbulence in the core. Shortly after the commencement of an imposed excursion of flow rate, additional turbulence is generated in the wall region and this propagates outwards at a speed characterized by the value of friction velocity associated with the initial Reynolds number. As time proceeds, further turbulence is generated and this propagates outwards at speeds which increase as the Reynolds number increases. Let us designate the time taken for the turbulence generated at $t = 0$ to propagate a distance y from the wall as τ_0, that for the turbulence generated at some time t later as τ and let us note that the τ will decrease with time at a rate which depends on the imposed acceleration. Now, turbulence generated at time t will arrive at the position under consideration at time $\tau + t$ and this function will vary in a manner which depends on the ramp rate of the excursion. If this is below a certain limit, $\tau + t$ will increase steadily with time. In this case, turbulence generated at $t = 0$ will always arrive at the location a distance y from the wall before any which is generated later and its arrival will mark the end of the delay period. Under such conditions, the delay in the response of turbulence at the location under consideration will be τ_0 and its value will depend on initial Reynolds number but not on ramp rate. The fact that no systematic variation of delay was observed as ramp rate was increased in the series of experiments with constant initial Reynolds number indicates that the above-mentioned limit was not reached in those experiments.

If the ramp rate of an imposed excursion of flow rate exceeds the limit referred to above, the function $\tau + t$ could initially decrease and reach a minimum value less than τ_0 at some time t_1. The new structure generated at time t_1 would then arrive at the position earlier than that generated at $t = 0$. Therefore, the delay would be reduced from τ_0 to $\tau_1 + t_1$ and this time would become shorter with the increase of the acceleration of the fluid. An example of an excursion in which this is the case will be discussed in § 4.4 where some additional results from the present study are presented for an excursion of shorter time period (2 s). In the extreme situation, when a step increase of flow rate is imposed, the delay time must be dependent on the ultimate flow rate. As mentioned earlier, this is exactly what was found by Maruyama *et al.* (1976) in the study of the response of turbulence to a stepwise increase in flow rate.

During the 'developing stage', the variation of turbulence quantities is controlled by the acceleration of the fluid and will be independent of the history of the flow variation. No matter what was the value of flow rate at which the excursion began, the development of the turbulence quantities in the developing stage will follow the same variation as long as the acceleration of the flow is the same. This was illustrated by the results shown in figures 18 and 19 from the series of experiments with constant ramp rate, which clearly showed that the data for the axial and radial components of the RMS turbulent fluctuations for various starting Reynolds numbers collapsed

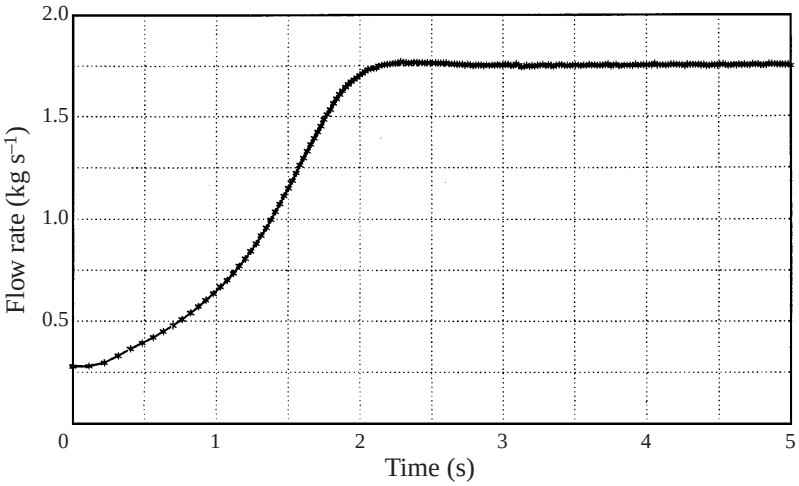

FIGURE 22. Flow rate variation in a 2 s time period ramp-up flow excursion test.

onto two different straight lines in the later stages of the ramp-up and ramp-down transients, respectively. At any instant, the turbulence properties at position y can be related to the flow which prevailed a period of time τ before. This time τ is equal to the time taken for the turbulence to propagate from y_0 to the position y. Taking U_τ as the characteristic speed of the propagation, τ will then be proportional to y/U_τ. Thus, the development of turbulence quantities in a transient flow might be approximated using pseudo-steady data and simply correcting for the local delay time τ using $\sqrt{2}y/U_{\tau 0}$. Since the delay time is not dependent on the acceleration of flow, for flow excursions with a range of ramp periods the time lag between the development of turbulence quantities in the transient flows will be the same. The difference between turbulence quantities in the various excursions and their corresponding pseudo-steady values will not, however, be the same (see figures 14 and 15). This is because, with different accelerations, the flow rates and therefore their pseudo-steady turbulence quantities are not the same in different excursions after the same period of time although the delay period is the same. The faster the transient, the larger will be the difference.

The propagation away from the wall of the response of turbulence in boundary layer flow to changes in curvature or streamwise pressure gradient has been found to occur in a manner which is similar to that in the present transient flow experiments, see for example, Baskaran *et al.* (1987) and Webster *et al.* (1996). In these studies, 'knee points', which indicated changes in turbulence structure, always appeared first near the wall. They gradually propagated towards the edge of the boundary layer as the flow proceeded downstream. Below the 'knee points', the stresses increased with downstream distance, which clearly indicated the arrival of new turbulence structure.

4.4. *The post-transient response*

In this subsection, we consider responses of local mean velocity and turbulence which can occur after an imposed excursion of flow rate has ended. Results from some additional experiments in which such measurements were obtained will be presented. These include results from ramp-up experiments in which the bulk velocity was increased from 0.139 m s^{-1} to 0.891 m s^{-1} over a time period of about 2 s ($Re_0 = 7000$, $Re_1 = 45\,200$ and $\gamma = 15.3$), in which data acquisition was extended for a period of

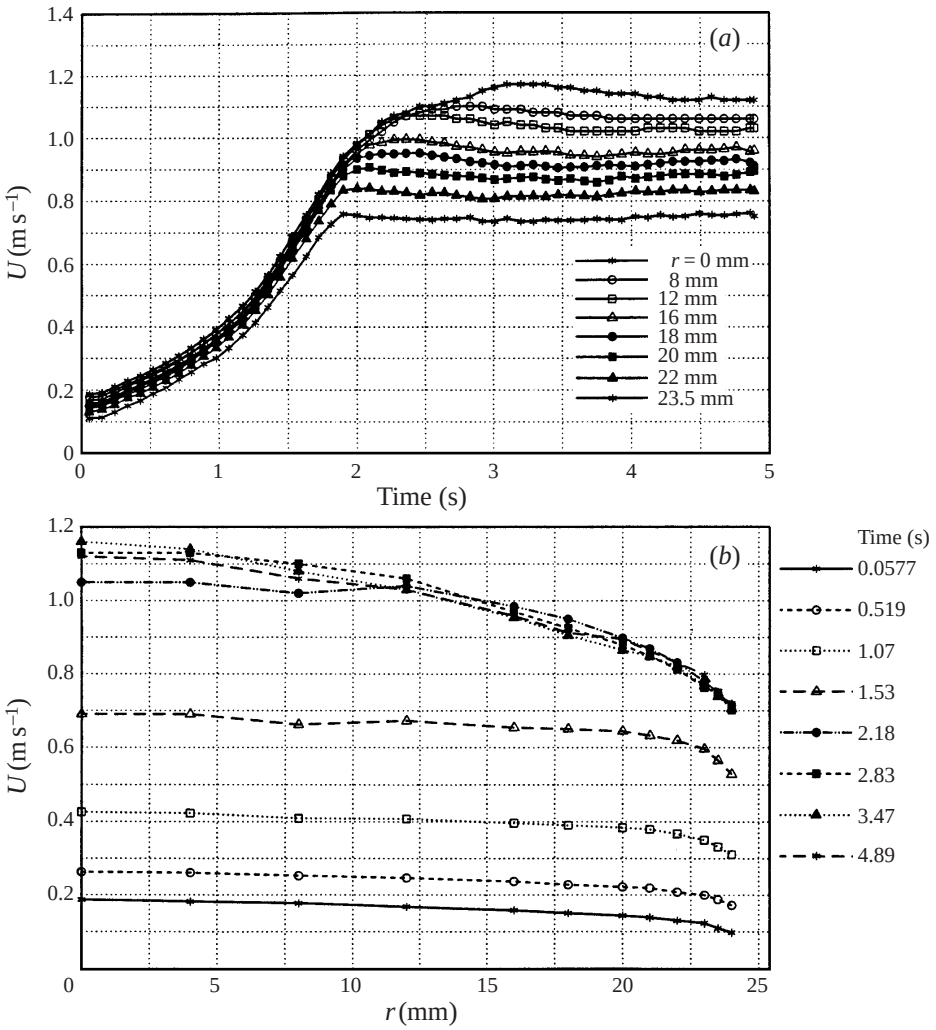

FIGURE 23. Variation of local mean velocity during and after a 2 s time period ramp-up flow excursion: (*a*) time variation, (*b*) profile development.

3 s after the end of the imposed flow excursion. Due to the mechanical limitations of the valve used, the acceleration of the flow could not be maintained constant during such a fast excursion, see figure 22. The results are nevertheless closely consistent with those presented earlier for linearly varying flow rate excursions of longer time period. Figures 23(*a*) and 23(*b*) show the time variation of local mean velocity and development of the velocity profiles, respectively. It can be seen that during most of the period of the imposed excursion, the local mean velocity in this experiment increased at a similar rate at all the radial locations for which data were obtained. Thus the flow accelerated in a slug-type manner. Later on, the velocity at locations near the wall stopped increasing and this tendency gradually extended towards the centre of the pipe. As can be seen from figure 22, the flow rate reached its final value 2.2 s after the start of the transient. Beyond that time, no further additional pressure gradient was imposed on the flow. However, the velocity continued to vary locally for about another 2 s. At the time that further increase of applied pressure ceased, the

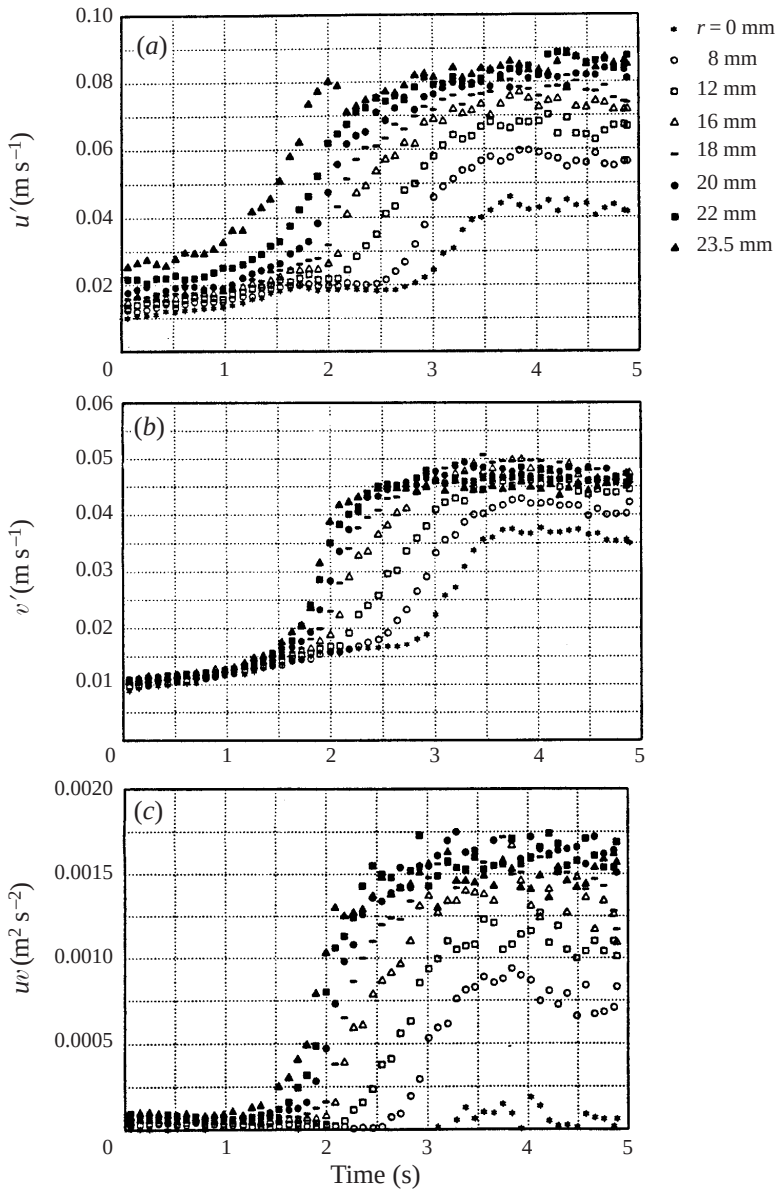

FIGURE 24. Variation of turbulence properties during and after a 2 s time period ramp-up transient: (*a*) RMS fluctuation of axial velocity component, (*b*) RMS fluctuation of radial velocity component, (*c*) turbulent shear stress.

velocity and turbulence fields still differed markedly from those of the corresponding steady flow and therefore the velocity profile continued to change.

The time variation of turbulence quantities for this excursion is shown in figure 24. A two-stage response is again clearly evident. At some locations, the delay extended beyond the end of the imposed excursion of flow rate. The delays in u' and v' at the centre of the pipe are about 3 s, about 1 s shorter than that found in the experiments presented earlier (§ 3.2). Thus the observation made on the basis of the experiments presented earlier that the delay in the response of turbulence in the core region does

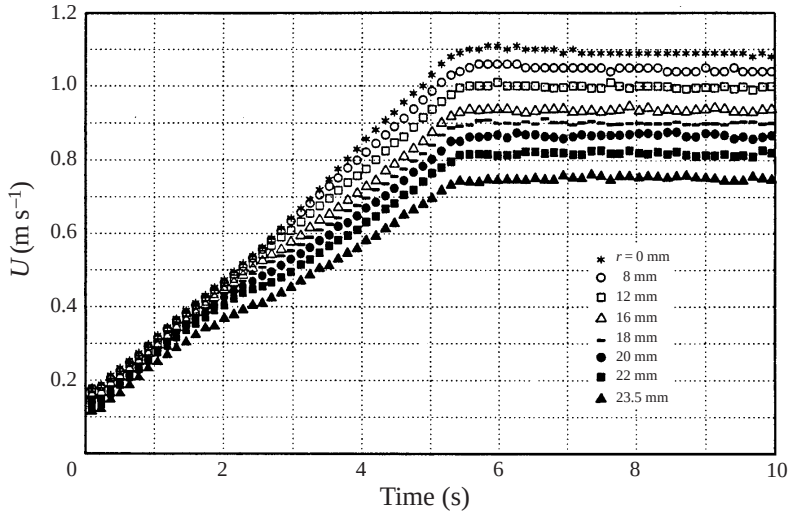

FIGURE 25. Variation of local mean velocity during and after a 5 s time period ramp flow excursion.

not depend on the time period of the ramp is no longer valid under the conditions of this faster transient. A detailed explanation of why this is so has been given in the preceding section. The turbulence field eventually settles down about 1.3 s after the end of the flow excursion.

Figures 25 and 26 show the time variations of local mean velocity and the turbulence components u' and v' for a 5 s time period ramp-up experiment for which data were collected for 5 s after the end of the imposed excursion of flow rate. It is apparent that the variations of both local mean velocity and turbulence which occur after the end of the transient are less significant than those in the 2 s transient discussed above. The additional pressure gradient needed to accelerate the flow in a 5 s transient is much smaller than that in a 2 s transient and therefore causes less distortion of both the flow and turbulence fields. At the end of the imposed excursion in the 2 s time period case, turbulence has only been responding for a short time in most parts of the flow field. In the core region, it is still within the delay stage and the turbulence quantities are still not very different from their starting values. Consequently, at the end of the excursion, the turbulence levels are far below those of the corresponding pseudo-steady condition. However, in the case of excursion of longer time period, five seconds have passed since the initiation of the transient and the turbulence has had a relatively long time to respond. The turbulence quantities have increased significantly, even at the centre of the pipe (where the delay period is about four seconds). Consequently, the difference between turbulence quantities at the end of the excursion of flow rate and the corresponding pseudo-steady-state values is much less than in the case of the excursion of time period of 2 s. However, it seems that the time needed for the flow and turbulence fields to eventually settle down is similar in both excursions (about 1.3 s).As argued earlier, this time scale is likely to be dependent on the final Reynolds number Re_1(45 200).

4.5. *Characterization of transient flow with ramp-type excursions of flow rate*

It is clear from the results and discussion presented here that delays in the response of turbulence to imposed variations of the mean flow field are an important feature of ramp-type transient turbulent flow. Three delays have been identified, namely

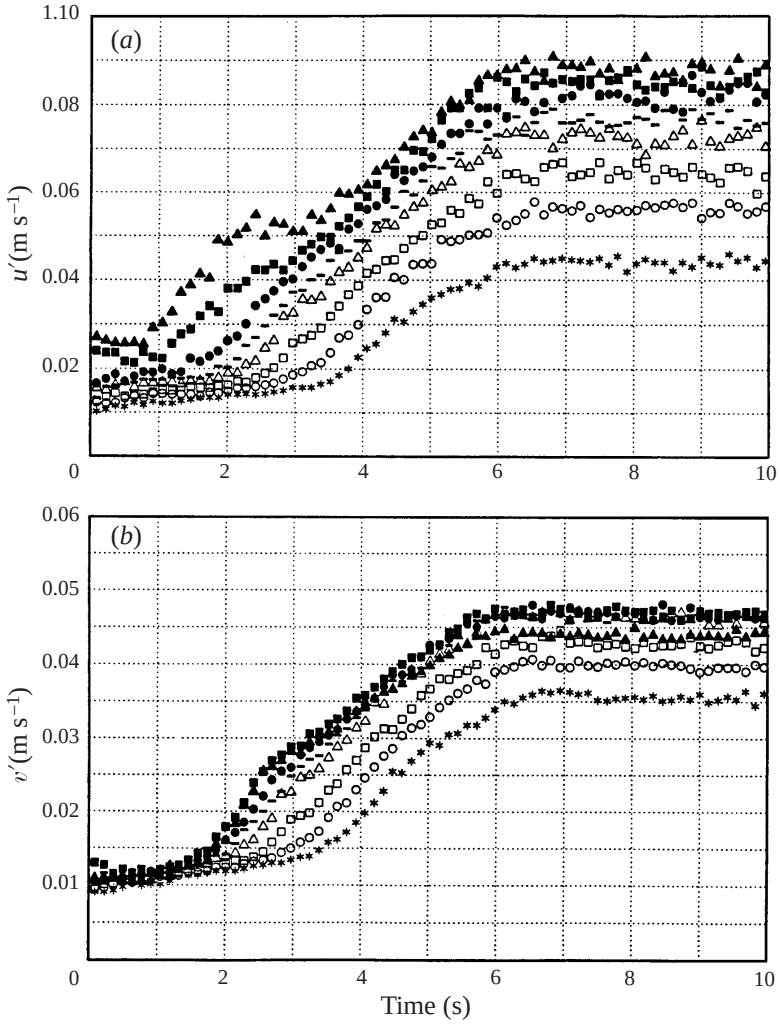

FIGURE 26. Variation of turbulent quantities during and after a 5 s time period ramp-up flow excursion: (*a*) RMS fluctuation of axial velocity component, (*b*) RMS fluctuation of radial velocity component. Symbols as in figure 25.

a delay in the response of turbulence production, a delay in the redistribution of turbulence among its three components and a delay associated with the propagation of turbulence radially. Of the three delays, the one associated with the radial propagation of turbulence is the most pronounced under the conditions of the present experiments.

The dimensionless parameter $\gamma[=(D/U_{\tau 0})((1/U_{b0})(\mathrm{d}U_b/\mathrm{d}t))]$ introduced in § 1.6 for the purpose of characterizing the ramp-type excursions of the present study was defined using a time scale $D/U_{\tau 0}$ associated with the propagation of turbulence from the wall to the centre of the core and a time scale for the imposed ramp $U_{b0}/(\mathrm{d}U_b/\mathrm{d}t)$. It can be shown that this represents the degree of departure of turbulence within the delay period from that for pseudo-steady flow. This can be seen by noting the fact that turbulent energy intensity $k^{1/2}/U_b$ is generally only a weak function of Reynolds number. To a first order of approximation, we can assume that $k^{1/2}/U_b$ remains constant during the period of an imposed transient. With this in mind, the ramp rate parameter

γ can be re-written as $((\mathrm{d}k/\mathrm{d}t)(R/U_\tau))/k$. In this expression, $\mathrm{d}k/\mathrm{d}t$ represents the rate of increase of turbulent kinetic energy of a corresponding pseudo-steady flow which would be associated with the imposed rate of increase of the flow rate. The ratio R/U_τ is the time scale associated with the propagation of turbulence from the wall to the centre of the pipe. The product of the two provides a measure of the difference which will develop during the delay period between the turbulent kinetic energy of the transient flow and the corresponding pseudo-steady flow. This represents the greatest departure of turbulence in the transient flow from its corresponding pseudo-steady value. After the delay period, turbulence starts to respond and the difference reduces. On dividing by the turbulent kinetic energy k, we obtain a relative measure of the difference.

Consequently, for $\gamma \gg 1$, we expect to see large deviations of turbulent energy in a transient flow from the corresponding values for pseudo-steady flow. The mean flow profiles will also depart from their pseudo-steady counterparts. Such flow is appropriately classified as a 'fast transient'. On the other hand, for $\gamma \ll 1$, the deviations will be small and the flow can be classified as a 'slow transient'. As an example, we can see from table 1 that γ for the 5, 20 and 90 ramp-up excursions of the present study takes values of 6.1, 1.5 and 0.34 respectively. Thus those excursions might be classified to be 'fast', 'intermediate' and 'slow', respectively. This is clearly consistent with the observed behaviour.

In the related study of Lefebvre (1987), the acceleration of the flow was large, but the initial flow rate was high. Consequently, the ramp rate parameter γ was only slightly in excess of unity. Thus one would only expect the deviations of turbulence from corresponding pseudo-steady values to be moderate. This was certainly so in the case of Lefebvre's results.

The corresponding scaling parameter used in studies of pulsating periodic flow is the turbulence Stokes number $\omega D/U_\tau$ proposed by Ramaprian & Tu (1983). This also is based on ideas of turbulence propagation.

As an alternative to γ a different ramp rate parameter can be defined based on the delay associated with turbulence production, using the time scale ν/U_τ^2 (a time scale associated with the inner turbulent layer). This leads to a parameter δ given by

$$\delta = \frac{\mathrm{d}U_b}{\mathrm{d}t}\frac{1}{U_{b0}}\frac{\nu}{U_{\tau 0}^2}. \tag{16}$$

This has similar physical basis to the parameters ω^+ and l^+ used by Mao & Hanratty (1986) and Tardu *et al.* (1994), respectively, for periodic flows.

As mentioned at the beginning of this section, the delay associated with the propagation of turbulence across the flow is the most pronounced of the delays which have been identified in the ramp-type flows under consideration here. Consequently, the ramp rate parameter γ is the appropriate one for characterizing the present flows. However, for ramp-up flows with very strong acceleration, in which the delay associated with the production of turbulence becomes significant, the parameter δ might be a more appropriate one. This point is also applicable in the case of periodic flow. Whereas the turbulence Stokes number $\omega D/U_\tau$ is suitable as a scaling parameter for some periodic transient flows, the parameters ω^+ and l^+ characterize periodic transient flows better when the frequency of the pulsation of the flow is high.

Finally, let us recall the parameters which are used for characterizing spatially accelerating flows. The two most common ones are

$$k = -\frac{\nu}{\rho U^3}\frac{\mathrm{d}p}{\mathrm{d}x} = \frac{\nu}{U^2}\frac{\mathrm{d}U}{\mathrm{d}x} \quad \text{and} \quad \Delta_p = \frac{\nu}{\rho U_\tau^3}\frac{\mathrm{d}p}{\mathrm{d}x} = -\frac{\nu}{U_\tau^2}\frac{\mathrm{d}U}{\mathrm{d}x}\left(\frac{C_f}{2}\right)^{1/2},$$

where U is the free-stream velocity in the case of a boundary layer flow and the mean velocity in the case of pipe flow. As can be seen Δ_p and k are related such that $\Delta_p = -(C_f/2)^{-3/2}k$. Other combinations of k and C_f of the form k/C_f and $k/C_f^{1/2}$ have also been proposed for data correlation, see for example, Kline *et al.* (1967), Patel & Head (1968) and Webster *et al.* (1996). In practice, the variation of C_f is generally small compared with that of k so that these different parameters are essentially similar.

For transient pipe flow, the following relation applies:

$$\frac{1}{2}\frac{\mathrm{d}U_b}{\mathrm{d}t} = -\frac{1}{2\rho}\frac{\mathrm{d}p}{\mathrm{d}x} + \frac{\tau_w}{\rho R}. \tag{17}$$

When the acceleration of a flow is moderate or strong, the first term on the right-hand side of (17) is much greater than the second and therefore

$$\frac{\mathrm{d}U_b}{\mathrm{d}t} \cong -\frac{1}{\rho}\frac{\mathrm{d}p}{\mathrm{d}x}. \tag{18}$$

The parameter δ defined in (16) can then be related to Δ_p and k as follows:

$$\delta = \frac{\mathrm{d}U_b}{\mathrm{d}t}\frac{1}{U_{b0}}\frac{\nu}{U_{\tau 0}^2} \approx -\frac{\nu}{\rho\, U_{\tau 0}^2}\frac{1}{U_{b0}}\frac{\mathrm{d}p}{\mathrm{d}x} = -\Delta_p\left(\frac{f}{2}\right)^{1/2} = k\left(\frac{f}{2}\right)^{-1}. \tag{19}$$

Thus, it can be seen that there is a connection between the ramp rate parameter δ and the parameters which are used for characterizing spatially accelerating flows.

5. Conclusions

This fundamental study of the mean flow and turbulence fields in ramp-type excursions of flow rate has yielded useful new information concerning transient turbulent flow and valuable insight into certain fundamental aspects of turbulence dynamics. The main conclusions can be summarized as follows:

(1) In fast ramp-type excursions of flows, the response of the mean flow field initially takes the form of a slug flow variation. The acceleration (deceleration) of the flow is then practically the same throughout the core and the boundary layer regions and the velocity gradient becomes steeper in a very thin region near the wall. The velocity profile distorts accordingly.

(2) A particularly interesting feature of the response of turbulence to imposed ramp-type excursions of flow rate is the occurrence of various delays. Three have been identified: a delay in the response of turbulence production, a delay in turbulence energy redistribution among its three components and a delay associated with the propagation of additional turbulence radially. As a result of these delays turbulence intensity is attenuated in an accelerating flow and is increased in a decelerating flow.

(3) On imposing a ramp-up flow excursion, the mean velocity field starts to respond first. The velocity gradient increases in a region very near the wall, the extent of which gradually grows with time. Until this region overlays the region where turbulence production peaks, there is little increase of turbulence. We therefore see a delay in the response of turbulence production. A time scale of ν/U_τ^2 is suggested for this delay. Its value is basically determined by the initial flow condition and is not dependent on the acceleration applied to the flow.

(4) In the wall region, the responses of the various components of turbulence are different. The axial component responds to an imposed transient with only a short delay whereas the radial and circumferential components each exhibit distinct two-stage responses with a longer delay which does not depend on the radial position. The difference in response reflects the process of redistribution of turbulent energy between the components through the action of pressure strain.

(5) The additional turbulent energy generated near the wall propagates outwards. The speed of the propagation is mainly dependent on the conditions prevailing when the additional structure was generated and can be related to U_τ. It therefore increases with the increase of the starting Reynolds number of the transient, but is not affected by the imposed acceleration of the flow except in the case of very fast transients. In this case, turbulence generated later may overtake that generated earlier in the course of propagating outwards and then a reduced delay is experienced.

(6) As a result of the time needed for propagation, the development of turbulence at positions away from the wall region exhibits a two-stage variation. During the early part of a transient, normal turbulent stresses respond slowly. The delay stage ends with the arrival of additional turbulence originating from the wall region after a period of time which is given by $\sqrt{2}y/U_\tau$. Then the developing stage begins. The response of each of the normal turbulent stresses in the core region is similar. This can be explained by the fact that the time scale for the process of the redistribution of turbulent energy between the three components is much smaller in this region than that for the propagation of turbulence.

(7) In the wall region, the response of the turbulent shear stress is similar to that of the radial and circumferential normal stresses. In the core region, the delay in its response is similar to those of the normal stresses. However, unlike the normal stresses, the shear stress remains completely unchanged during the delay.

(8) Inertia plays an important role in the momentum balance even when the imposed excursion of flow rate is slow and little effect of the transient is seen on the mean flow and turbulence fields. As the shear stress builds up during a ramp-up flow excursion, the relative magnitude of the inertial term reduces, but it still remains significant in the momentum balance even in the later stages of a transient. The direct effect of inertia on the mean flow field is only felt in the early stages of faster transients.

(9) The appropriate dimensionless groups for similarity and scaling in the case of ramp-type transient turbulent flows of the kind studied here have been identified as the initial and final Reynolds numbers $Re_0(=(\rho U_{b0}D)/\mu)$ and $Re_1(=(\rho U_{b1}D)/\mu)$ and a ramp rate parameter $\gamma(=(\mathrm{d}U_b/\mathrm{d}t)(1/U_{b0})(D/U_{\tau 0})$. The latter can be expressed as the ratio of two time scales, $D/U_{\tau 0}$ and $U_{b0}/(\mathrm{d}U_b/\mathrm{d}t)$. The first of these is associated with turbulence propagation and the other with the imposed ramp. Significant delays in the response of turbulence are to be expected during a flow excursion if this parameter is much greater than unity. If it is very much less than unity, conditions of pseudo-steady transient flow will prevail.

(10) An alternative parameter $\delta(=(\mathrm{d}U_b/\mathrm{d}t)(1/U_{b0})(\nu/U_{\tau 0}^2))$ is proposed for very fast transients. This is based on the delay in the response of turbulence production rather than the time scale for turbulence propagation.

(11) The response of turbulence in ramp-up transient flow exhibits some similarities to that in boundary layer flow with a falling streamwise pressure gradient. Similarly, the response of turbulence in ramp-down transient flow exhibits some similarities to the behaviour in boundary layer flow with a rising streamwise pressure gradient.

REFERENCES

Baskaran, V., Smits, A. & Joubert, P. N. 1987 A turbulent flow over a curved hill, Part 1. Growth of an internal boundary layer. *J. Fluid Mech.* **182**, 47–83.

Binder, G. & Kueny, J. L. 1981 Measurements of the periodic velocity oscillations near the wall in unsteady turbulent channel flow. In *Turbulent Shear Flow 3* (ed. L. Bradbury, F. Durst, B. Launder, G. Schmidt & J. N. Whitelaw), pp. 6–17. Springer.

Binder, G., Tardu, S., Blackwelder, R. F. & Kueny, J. L. 1985 Large amplitude periodic oscillations in the wall region of a turbulent channel flow. *Fifth Symp. on Turbulent Shear Flows, Cornell University, Ithaca, NewYork.*

Blackwelder, R. F. & Haritonidis, J. H. 1983 Scaling of the bursting frequency in turbulent boundary layers. *J. Fluid Mech.* **132**, 87–103.

Blackwelder, R. & Kovasznay, L. S. G. 1972 Large-scale motion of a turbulent boundary layer during relaminarization. *J. Fluid Mech.* **53**, 61–83.

Blondeaux, P. & Colombini, M. 1985 Pulsating turbulent pipe flow. *Fifth Symp. on Turbulent Shear Flows, Cornell University, Ithaca, New York.*

Burnel, S., Raelison, J. C. & Thomas, J. M. 1990 Radial distribution of the Reynolds stress in a turbulent pulsating flow in a pipe. In *Engineering Turbulence Modelling and Experiments* (ed. W. Rodi & Y. Ganic), pp. 419–427. Elsevier.

Burnel, S., Raelison, J. C. & Thomas, J. M. 1991 Radial distribution of the Reynolds stress in a turbulent pulsating flow in a pipe. *Euromech Colloquium 272 Response of Shear Flows to Imposed Unsteadiness, Aussois, France.*

Cook, W. J., Murphy, J. D. & Owen, F. K. 1985 An experimental and computational study of turbulent boundary layers in oscillating flows. *Fifth Symp. on Turbulent Shear Flows, Cornell University, Ithaca, New York.*

Cotton, M. A. & Ismael, J. O. 1991 An examination of periodic turbulent pipe flow using a low-Reynolds-number k-ϵ, turbulence model. *Eighth Symp. on Turbulent Shear Flows, Technical University of Munich, Germany.*

Cousteix, J., Javelle, J. & Houdeville, R. 1981 Influence of Strouhal number on the structure of a flat plate turbulent boundary layer. *Third Symp. on Turbulent Shear Flows, University of California, Davis, USA.*

Durst, F., Martinuzzi, R., Sender, J. & Thevenin, D. 1994 LDA-measurements of mean velocity, RMS-values and higher order moments of turbulence intensity fluctuations in flow fields with strong velocity gradients. *Seventh Intl Symp. on Applications of Laser Techniques to Fluid Mechanics*, Paper 5.1, pp. 1–6.

Kataoka, K., Kawabata, T. & Miki, K. 1975 The start-up response of pipe flow to a step change in flow rate. *J. Chem. Engng Japan* **8**, 266–271.

Kirmse, R. E. 1979 Investigations of pulsating turbulent pipe flow. *Trans. ASME* **101**, 436–442.

Kita, Y., Adachi, Y. & Hirose, K. 1980 Periodically oscillating turbulent flow in a pipe. *Bull. JSME* **23**, 656–664.

Kline, S. J., Reynolds, W. C., Schraub, F. A. & Runstadler, P. W. 1967 The structure of turbulent boundary layers. *J. Fluid Mech.* **30**, 741–773.

Kurokawa, J. & Morikawa, M. 1986 Accelerated and decelerated flows in a circular pipe (1st report, velocity profiles and friction coefficient). *Bull. JSME* **29**, 758–765.

Launder, B. E. & Sharma, B. I. 1974 Application of the energy-dissipation model of turbulence to the calculation of flow near a spinning disc. *Lett. Heat Mass Transfer* **1**, 131–138.

Lawn, C. J. 1971 The determination of the rate of dissipation in turbulent pipe flow. *J. Fluid Mech.* **48**, 477–505.

Lefebvre, P. J. 1987 Characterization of accelerating pipe flow. PhD thesis, University of Rhode Island.

Mao, Z. & Hanratty, T. J. 1986 Studies of the wall shear stress in a turbulent pulsating pipe flow. *J. Fluid Mech.* **170**, 545–564.

Maruyama, T., Kuribayashi, T. & Mizushina, T. 1976 The structure of the turbulence in transient pipe flows. *J. Chem. Engng Japan* **9**, 431–439.

Mizushina, T., Maruyama, T. & Hirasawa, H. 1975 Structure of the turbulence in pulsating pipe flows. *J. Chem. Engng Japan* **8**, 210–216.

Mizushina, T., Maruyama, T. & Shiozaki, Y. 1973 Pulsating turbulent flow in a tube. *J. Chem. Engng Japan* **6**, 487–494.

Muck, K. C., Hoffmann, P. H. & Bradshaw, P. 1995 The effect of convex surface curvature on turbulent boundary layers. *J. Fluid Mech.* **161**, 347–369.

Murphy, J. D. & Prenter, P. M. 1981 A hybrid computing scheme for unsteady turbulent boundary layers. *Proc. Third Symp. on Turbulent Shear Flows, Pennsylvania State University,* pp. 8.26–8.34.

Narayanan, M. A. & Ramjee, V. 1969 On the criteria for reverse transition in a two-dimensional boundary layer flow. *J. Fluid Mech.* **35**, 225–241.

Ohmi, M., Usui, T., Tanaka, O. & Toyama, M. 1976 Pressure and velocity distributions in pulsating turbulent pipe flow, part 1: Theoretical treatments. *Bull. JSME* **19**, 307–313.

Ohmi, M., Kyomen, S. & Usui, T. 1978 Analysis of velocity distribution in pulsating turbulent pipe flow with time-dependent friction velocity. *Bull. JSME* **21**, 1137–1143.

Oldengarm, O., Krieken, A. H. van & Klooster, H. W. van der 1975 Velocity profile measurements in a liquid film flow using the laser Doppler technique. *J. Phys.* E: *Sci. Instru.* **8**, 203–205.

Patel, V. C. & Head, M. R. 1968 Reversion of turbulent to laminar flow. *J. Fluid Mech.* **34**, 371–392.

Ramaprian, B. R. & Tu, S. W. 1980 An experimental study of oscillatory pipe flow at transitional Reynolds numbers. *J. Fluid Mech.* **100**, 513–544.

Ramaprian, B. R. & Tu, S. W. 1983 Fully developed periodic turbulent pipe flow. Part 2. The detailed structure of the flow. *J. Fluid Mech.* **137**, 59–81.

Sano, M. & Asako, Y. 1993 Fluid flow and heat transfer in a periodically diverging-converging turbulent duct flow. *Intl J. JSME* **36**, 207–213.

Schwarz, A. C. & Plesniek, M. W. 1996 Convex turbulent boundary layers with zero and favourable pressure gradients. *Trans. ASME J. Fluids Engng* **118**, 787–794.

Shemer, L. & Kit, E. 1984 An experimental investigation of the quasisteady turbulent pulsating flow in a pipe. *Phys. Fluids* **27**, 72–76.

Shemer, L. & Wygnanski, I. 1981 On the pulsating flow in pipe. *Third Symp. on Turbulent Shear Flows, University of California,* Davis, pp. 8.13–8.18.

Shemer, L., Wygnanski, I. & Kit, E. 1985 Pulsating flow in a pipe. *J. Fluid Mech.* **153**, 313–337.

Spencer, E. A., Heitor, M. V. & Castro, I. P. 1995 Intercomparison of measurements and computations of flow through a contraction and a diffuser. *Flow Meas. Instrum.* **6**, 3–14.

Tanaka, T & Yabuki, H. 1986 Laminarization and reversion to turbulence of low Reynolds number flow through a converging to constant area duct. *Trans. ASME J. Fluids Engng* **108**, 325–330.

Tardu, S. F., Binder G. & Blackwelder, R. F. 1994 Turbulent channel flow with large amplitude. *J. Fluid Mech.* **269**, 109–151.

Tu, S. W. & Ramaprian, B. R. 1983 Fully developed periodic turbulent pipe flow. Part 1. Main experimental results and comparison with predictions. *J. Fluid Mech.* **137**, 31–58.

Webster, D. R., Degraaff, D. B. & Eaton, J. K. 1996 Turbulence characteristics of a boundary layer over a two-dimensional bump. *J. Fluid Mech.* **320**, 53–69.